AD-A176 896 OXYGEN PHOTOABSORPTION(U) ADELAIDE UNIV (AUSTRALIA) DEPT OF PHYSICS A J BLAKE 14 OCT 83 AFGL-TR-84-0025 AFOSR-78-3716 1/1

UNCLASSIFIED F/G 7/4 NL

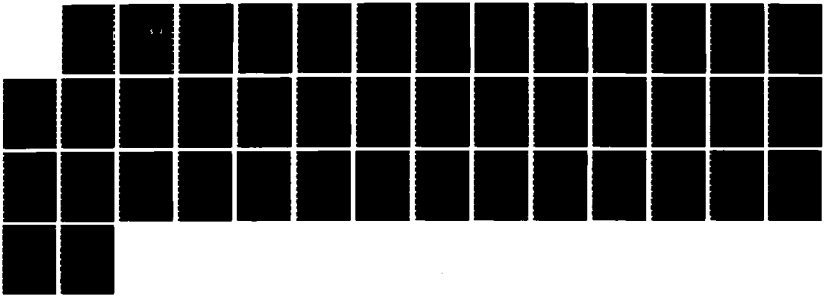

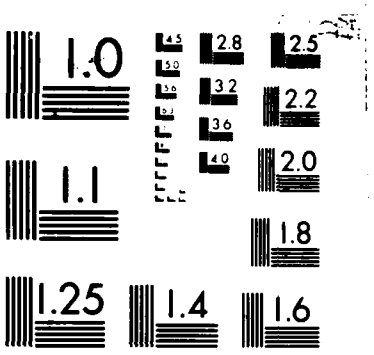

(12)

AFGL-TR-84-0025

Oxygen Photoabsorption

Alastair J. Blake

University of Adelaide
Department of Physics
Adelaide, South Australia 5000
AUSTRALIA

14 October 1983

Final Report
15 September 1978 - 31 December 1982

APPROVED FOR PUBLIC RELEASE; DISTRIBUTION UNLIMITED

AIR FORCE GEOPHYSICS LABORATORY
AIR FORCE SYSTEMS COMMAND
UNITED STATES AIR FORCE
HANSCOM AIR FORCE BASE, MASSACHUSETTS 01731

"This technical report has been reviewed and is approved for publication"

Robert E. Huffman

ROBERT E. HUFFMAN
Contract Manager

Robert E. Huffman

ROBERT E. HUFFMAN
Chief,
UV Surveillance & Remote Sensing Branch

FOR THE COMMANDER

ROBERT A. SKRIVANEK
Director
Ionospheric Physics Division

This report has been reviewed by the ESD Public Affairs Office (PA) and is releasable to the National Technical Information Service (NTIS).

Qualified requestors may obtain additional copies from the Defense Technical Information Center. All others should apply to the National Technical Information Service.

If your address has changed, or if you wish to be removed from the mailing list, or if the addressee is no longer employed by your organization, please notify AFGL/DAA, Hanscom AFB, MA 01731. This will assist us in maintaining a current mailing ist.

Do not return copies of this report unless contractual obligations or notices on a specific document requires that it be returned.

Unclassified

SECURITY CLASSIFICATION OF THIS PAGE (When Data Entered)

REPORT DOCUMENTATION PAGE		READ INSTRUCTIONS BEFORE COMPLETING FORM
1. REPORT NUMBER AFGL-TR-84-0025	2. GOVT ACCESSION NO. A176	3. RECIPIENT'S CATALOG NUMBER 896
4. TITLE (and Subtitle) OXYGEN PHOTOABSORPTION		5. TYPE OF REPORT & PERIOD COVERED Final 15 Sept. 1978-31 Dec. 1982
		6. PERFORMING ORG. REPORT NUMBER
7. AUTHOR(s) ALASTAIR J. BLAKE		8. CONTRACT OR GRANT NUMBER(s) AFOSR - 78 - 3716
9. PERFORMING ORGANIZATION NAME AND ADDRESS University of Adelaide, Adelaide, South Australia Australia, 5000		10. PROGRAM ELEMENT, PROJECT, TASK AREA & WORK UNIT NUMBERS 61102F 2303G1AH
11. CONTROLLING OFFICE NAME AND ADDRESS AFOSR (PKZA) Building 410 Bolling, AFB, DC 20332		12. REPORT DATE 14 October 1983 13. NUMBER OF PAGES 42
14. MONITORING AGENCY NAME & ADDRESS (if different from Controlling Office) Air Force Geophysics Laboratory Hanscom AFB, Massachusetts 01731 Contract Manager: R. E. Huffman/LIU		15. SECURITY CLASS. (of this report) UNCLASSIFIED 15a. DECLASSIFICATION DOWNGRADING SCHEDULE

16. DISTRIBUTION STATEMENT (of this Report)

Approved for public release; distribution unlimited.

17. DISTRIBUTION STATEMENT (of the abstract entered in Block 20, if different from Report)

18. SUPPLEMENTARY NOTES

19. KEY WORDS (Continue on reverse side if necessary and identify by block number)

Ultraviolet, photoabsorption, oxygen, Schumann-Runge system.

20. ABSTRACT (Continue on reverse side if necessary and identify by block number)

Results of a study of photoabsorption in the Schumann-Runge system of molecular oxygen are reported. In the region of the Schumann-Runge continuum the temperature dependence of the photoabsorption cross-section has been measured and compared with theoretical calculations. In the band system measurements of the oscillator strengths and pre-dissociation widths of absorption lines have been made. These measurements can be applied to detailed modelling the absorption of solar ultraviolet radiation in the atmosphere.

DD FORM 1 JAN 73 1473 EDITION OF 1 NOV 65 IS OBSOLETE

Unclassified

SECURITY CLASSIFICATION OF THIS PAGE (When Data Entered)

TABLE OF CONTENTS

INTRODUCTION

The absorption of solar ultraviolet radiation by molecular oxygen is of fundamental importance in the atmosphere because it provides a mechanism for energy transfer in the atmosphere and, because of photodissociation of the oxygen molecule, it supplies the atomic oxygen that is crucial in the photochemical processes by which ozone is produced. Calculation of the rate of production of atomic oxygen as a function of altitude in the atmosphere involves detailed modelling of the complex photoabsorption process of molecular oxygen. Such an absorption model is also needed for the determination of molecular oxygen densities from absorption measurements in the atmosphere, and for the interpretation of measurements of airglow, aurora and other radiation that is observed through the oxygen of the atmosphere.

This project has involved measurements in the wavelength region from 140 nm to 200 nm. The features of the oxygen photoabsorption spectrum in this region are the Schumann-Runge dissociation continuum and the predissociated Schumann-Runge band system. There have been numerous studies of this spectrum, but advances in atmospheric sciences have demanded more detailed data. The emphasis of the work reported here is on an improved understanding of the fundamental absorption processes as a basis for detailed modelling of atmospheric absorption of solar ultraviolet radiation.

METHODS

Laboratory measurements of photoabsorption have been made using the University of Adelaide 6.65 m vacuum ultraviolet monochromator and a range of absorption cells with lengths varying

from 1 cm to 1 m. The temperature of the sample gas was varied over the range 100K to 600K. In addition to the laboratory work, theoretical calculations were made in which the Schroedinger equation for a vibrating-rotating molecule was solved and quantities such as the absorption cross-section, absorption-line oscillator strength and predissociation line width were computed. An important feature of the work was the combination of laboratory measurement and theoretical calculation to obtain new information about the absorption processes.

RESULTS

The work may be divided into three parts : a study of the Schumann-Runge continuum region, a study of the Schumann-Runge bands, and the modelling of atmospheric absorption processes. Detailed accounts of the work are contained in the Appendix where copies of published papers that resulted from the project are reproduced.

Schumann-Runge continuum

Measurements of the temperature dependence of the photo-absorption cross-section between 140 nm and 175 nm were compared with theoretical calculations and new data about the transition moment for the Schumann-Runge transition and the upper state potential curve were obtained. The details of this work are given in part A of the Appendix.

The temperature dependence data were applied to a re-analysis of atmospheric absorption measurements to extract the atmospheric oxygen density profile. The effects of temperature dependence in the analysis are described in part B of the Appendix.

At wavelengths larger than 175 nm a highly temperature

dependence component of the Schumann-Runge continuum underlies the band system. Measurements and calculations of this continuum are given in part C of the Appendix.

Schumann-Runge bands

Oscillator strengths and predissociation line-widths for absorption lines in the band system were measured using a curve-of-growth method. The results are given in part D of the Appendix.

Atmospheric absorption

All of the data obtained during the project has contributed to an improved model for calculation of photoabsorption by oxygen in the atmosphere. An example of the application of that model is given in part E of the Appendix to illustrate the accuracy with which the model reproduces the details of the absorption spectrum.

CONCLUSION

The work carried out during this project has produced new laboratory data, and by combining them with theoretical calculations of photo-absorption by molecular oxygen an improved model of the absorption processes has been obtained. This model can be used to compute dissociation rates for oxygen in the atmosphere and atmospheric transmittance spectra that can be used in the analysis of either high resolution or broad band observations of ultra-violet radiation that is transmitted through the atmosphere.

REFERENCES

Reprints of published papers that have resulted from the project.

A. Gibson, S.T., H.P.F. Gies, A.J. Blake, D.G. McCoy, and P.J. Rogers, Temperature dependence in the Schumann-Runge photoabosprtion continuum of oxygen, J. Quant. Spectrosc. Radiat. Transfer, In Press, 1983.

B. J.L. Lean and A.J. Blake, The effect of temperature on thermospheric molecular oxygen absorption in the Schumann-Runge continuum, J. Geophys. Res., 86, 211, 1981.

C. Gies, H.P.F., S.T. Gibson, A.J. Blake, and D.G. McCoy, The Schumann-Runge continuum of oxygen at wavelengths greater than 175 nm, J. Geophys. Res., 87, 8307-8310, 1982.

D. Gies, H.P.F., S.T. Gibson, D.G. McCoy, and A.J. Blake, Experimentally determined oscillator strengths and linewidths for the Schumann-Runge band system of molecular oxygen - III. The (7-0) to (19-0) bands, J. Quant. Spectrosc. Radiat. Transfer, 26, 469-481, 1981.

E. Gibson, S.T., H.P.F. Gies, A.J. Blake, and D.G. McCoy, Transmittance of the atmosphere in the (8-0) and (9-0) Schumann-Runge bands of oxygen, J. Geophys. Res., 88, 500-502, 1983.

J. Quant. Spectrosc. Radiat. Transfer Vol. 00, No. 00,
pp. 0000-0000, 1983. Printed in Great Britain

TEMPERATURE DEPENDENCE IN THE SCHUMANN–RUNGE PHOTOABSORPTION CONTINUUM OF OXYGEN

S. T GIBSON, H. P. F. GIES, A. J. BLAKE, D. G. MCCOY, and P. J. ROGERS
Department of Physics, University of Adelaide, Adelaide, South Australia 5001, Australia

(*Received* 9 *March* 1983)

Abstract—The photoabsorption cross section in the Schumann-Runge continuum of oxygen has been measured with high precision over the wavelength region 140–174 nm at temperatures in the range 295–575 K. Models for the upper state potential and the electronic transition moment were used in the calculation of the cross section and its temperature dependence. By comparing this theoretical cross section with measured values, curves for the upper state potential and the transition moment in the continuum region have been obtained independently for the first time.

INTRODUCTION

The photoabsorption cross section for the Schumann–Runge system of molecular oxygen, corresponding to the transition $X^3\Sigma_g^- - B^3\Sigma_u^-$, has its maximum strength in the dissociation continuum which extends from the limit of the band system at 175.05 to about 125 nm. Atmospheric absorption of solar radiation in this wavelength region is important because it provides the main source of oxygen atoms in the lower thermosphere and because measurments of atmospheric photoabsorption in this wavelength region can be used to determine the molecular oxygen density profile in the 100–200 km altitude region.

Measurements of the photoabsorption cross section in the Schumann–Runge continuum at room temperature have been made by many investigators.[1-14] Hudson[14] has made a critical review of these measurements. Evans and Schexnayder[8] have made a theoretical investigation of the temperature dependence of the cross section and presented measurements made at very high temperatures which are mainly of astrophysical interest. Measurements of the cross section at temperatures of 300, 600, and 900K have been reported by Hudson *et al.*[11] but these were limited to wavelengths greater than 160 nm at 600K and 173 nm at 900K. Carver *et al.*[15] and Weeks[16] have referred to the effects of temperature dependence on determinations of atmospheric oxygen densities using photoabsorption measurements in the Schumann–Runge continuum. A re-analysis of atmospheric absorption data based on measurements of the temperature dependence of the cross section (Lean and Blake[17]) has shown that the derived densities are smaller by as much as 20% than those obtained using the room temperature cross section.

The purpose of this paper is to report new measurements of temperature dependence in the Schumann–Runge continuum and to demonstrate that considerable insight into the shape of the upper state potential and the electronic moment for this transition can be obtained from a careful analysis of the data. These are the first measurements to be reported that make such an analysis possible.

EXPERIMENTAL MEASUREMENTS

Absorption measurements were made with gas samples at temperatures in the range 295 to 575K. Measurements were made using a 3 cm absorption cell which was electrically heated to temperatures up to 600 K. The cell was machined from an aluminium block and was fitted with flanged lithium fluoride windows. Thermocouples were used to monitor the cell temperature and to control a servo system which stabilised the cell at a constant temperature. This cell is illustrated in Fig. 1, where radiation baffling, which minimised radiation losses, has been omitted. The gas pressure was maintained at a constant value by a servo controlled needle

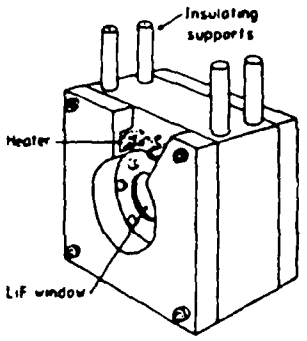

Fig. 1. The construction of the high temperature absorption cell. A radiation shield which surrounds the cell is not shown.

valve using the output from a capacitance manometer. Measurements were made at a resolution better than 0.01 nm using a 6.7 m monochromator equipped with a hydrogen discharge lamp. The incident and transmitted beams were monitored simultaneously and the relative sensitivity of the two detectors was checked before each run by evacuating the absorption cell. This experimental arrangement has already been discussed.[18].

The measured values of the cross section as a function of temperature at wavelengths of 149 and 165 nm that are shown in Fig. 2 illustrate the temperature-dependent behaviour of the cross section. It can be seen that both positive and negative temperature dependence occur at different wavelengths. The temperature dependence was determined throughout the wavelength range 140–174 nm by making measurements at temperatures of 300 and 575K. The measured cross sections are listed in Table 1, and the temperature coefficient, defined as $100\ (\sigma_{575} - \sigma_{300})/\sigma_{300}$, is shown in Fig. 3.

In determining the temperature dependence of the cross section, considerable care was taken to ensure that the relative cross sections were measured with high accuracy. Thus, while the values shown in Table 1 may have systematic errors as large as 5% due to uncertainties in the cell length and pressure-gauge calibration, the effect of the systematic errors is greatly reduced when calculating the temperature dependence of the cross section. The random error is typically 0.2%, arising mainly from photon-counting statistics and small wavelength drifts in the monochromator. This high precision is needed to ensure that accurate values are obtained for the change in the cross section with temperature. The statistical error was reduced to a small value by counting for an adequate time, and the effects of wavelength drift were reduced by making frequent checks of the wavelength using emission lines in the lamp spectrum as a reference. Beer's law behaviour of the cross section was tested by making measurements at a series of pressures and the cross sections listed are the result of many individual measurements.

THEORY

The source of the temperature dependence in the cross section and its relationship with fundamental molecular parameters can be understood from a simplified argument in which the rotational structure of the molecule is ignored. In this approximation, the absorption cross section for molecules in the vibrational state v'' is[19]

$$\sigma_{v''}(\lambda) = [\pi/(3\epsilon_0 hcg''\lambda)] \left| \int_0^\infty \Psi_{v''}(r) R_e(r) \Psi_E(r)\, dr \right|^2, \qquad (1)$$

where $g'' = (2 - \delta_{0v''})(2S + 1)$ is the statistical weight of the initial state, $\psi_{v''}$ is the normalised initial state vibrational wave function, ψ_E is the normalised final state continuum wave function, R_e is the electronic transition moment, λ is the wavelength of the absorbed radiation for the transition to a final state of energy E, and r is the internuclear distance. The wavefunctions are found by solving the Schrödinger equation using the potential $V_0(r)$ for the corresponding

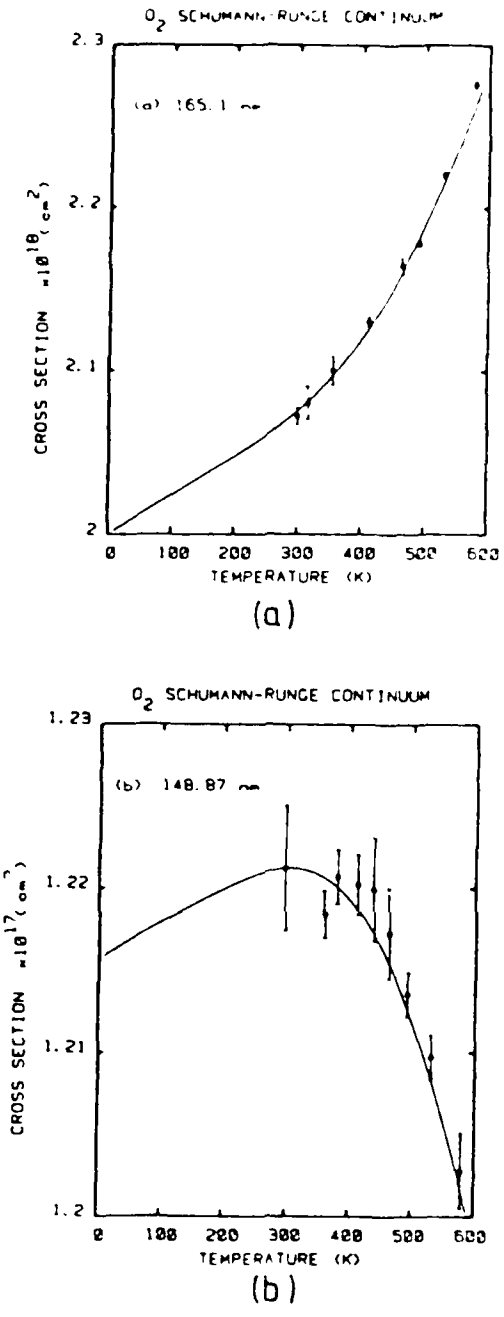

Fig. 2. The temperature dependence of the cross section in the Schumann-Runge continuum at wavelengths of (a) 165.1 nm and (b) 148.87 nm. The points are from experimental measurements and the curve was calculated using models for the molecular potentials and transition moment. The positive coefficient evident at temperatures less than 300K in both curves is a rotational effect.

electronic state of the molecule. At temperature T, the total absorption cross section is[20]

$$\sigma_T(\lambda) = \left(\sum_i \sigma_i(\lambda)\, e^{-G_i/kT}\right) \Big/ \left(\sum_i e^{-G_i/kT}\right), \tag{2}$$

where G_i is the initial state vibrational excitation energy.

Neither the form of the upper state potential curve in the region above the dissociation limit nor the form of the transition moment are well known. Allison *et al.*[20] have calculated curves

Table 1. Absorption cross sections in the Schumann-Runge continuum for temperatures of 295K and 575K in units of 10^{-18} cm^2. The errors quoted are statistical and do not include systematic errors

λ, nm	σ_{295}	σ_{575}
140.03	139.51±0.33	137.72±0.34
141.04	141.33±0.30	139.60±0.38
142.02	138.55±0.29	137.87±0.26
143.00	139.67±0.42	136.88±1.32
144.00	140.99±0.27	138.03±0.50
144.98	138.46±0.21	135.27±0.57
146.15	134.19±0.22	131.58±0.36
147.07	130.95±0.54	128.77±0.47
147.90	128.75±0.26	126.39±0.42
148.87	122.12±0.38	120.28±0.23
150.00	114.11±0.41	113.10±0.27
151.10	106.94±0.22	106.37±0.30
152.10	100.17±0.22	99.37±0.26
153.02	93.97±0.18	93.48±0.25
153.98	87.12±0.26	86.99±0.24
155.10	78.66±0.17	78.57±0.30
156.08	71.32±0.13	71.60±0.14
157.05	64.35±0.11	65.30±0.14
158.03	57.67±0.12	58.82±0.15
158.95	51.48±0.08	52.93±0.15
160.10	44.21±0.07	45.89±0.07
161.01	39.29±0.12	40.86±0.07
162.04	33.83±0.06	35.53±0.06
163.00	29.22±0.04	31.07±0.06
164.10	24.60±0.05	26.45±0.04
165.10	20.72±0.05	22.74±0.07
166.00	17.73±0.04	19.62±0.03
167.02	14.74±0.03	16.57±0.04
168.00	12.24±0.02	14.04±0.03
169.00	9.93±0.02	11.70±0.04
170.00	8.12±0.01	9.73±0.02
171.00	6.50±0.03	7.96±0.02
172.00	5.23±0.01	6.56±0.04
173.00	4.16±0.02	5.37±0.01
174.00	3.29±0.01	4.35±0.01

for σ_0, σ_1, and σ_2 by making plausible assumptions about the potential and the transition moment such that σ_0 was a good fit to the measured cross section at room temperature.

It is clear that measurement of the total cross section at a single temperature cannot yield information which would enable independent determination of the upper state potential and transition moment. Measurements of the temperature dependence of the cross section can be used to provide this additional information in the following way.

For temperatures up to 600K, only the two lowest vibrational levels have a significant population and Eq. (2) can be truncated to give

$$\sigma_T(\lambda) = (\sigma_0 + \sigma_1 e^{-G_1/kT})/(1 + e^{-G_1/kT}). \tag{3}$$

The cross section measurements at 300 and 600K listed in Table 1 can then be used to solve for values of σ_0 and σ_1.

It can be shown from Eq. (3) that the temperature dependence of the cross section in this temperature range depends mainly on the ratio σ_1/σ_0. Since the electronic transition moment R_e in Eq. (1) is expected to vary slowly with r, this ratio will depend only weakly on the form of R_e. However, in general σ_1/σ_0 depends on the form of the upper state potential curve, and calculation of the temperature dependence of the cross section at any wavelength in the continuum is most sensitive to the position of the potential curve at an energy near the energy of the final state. A comparison of calculations made, using Eqs. (1) and (2), with measurements of the temperature dependence as a function of wavelength would allow assumptions about the form of the potential curve to be tested. The assumed form for the electronic transition moment can be tested by comparing the measured and calculated curves for the total cross sections at a particular temperature. In this way, measurements of the cross section and its temperature dependence in the continuum allow otherwise inaccessible information about the potential curve and the transition moment to be obtained.

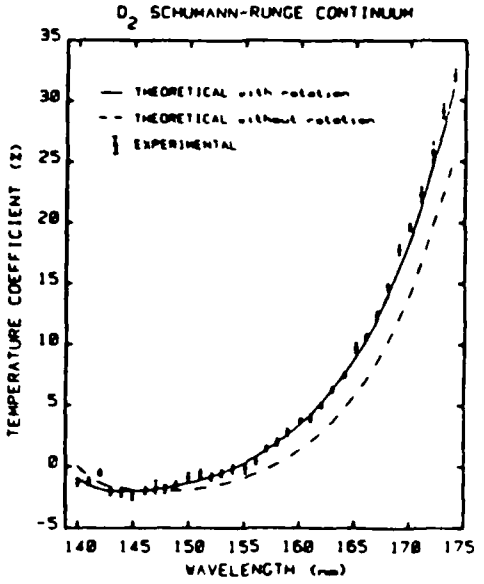

Fig. 3. The temperature coefficient of the Schumann-Runge continuum cross section. The curves were calculated using models for the molecular potentials and transition moment. In one curve, the rotational structure of the molecule has been ignored.

The preceding discussion was simplified by ignoring the rotational structure of the molecule which, in fact, has a very significant effect on the calculation of the cross section through the centrigugal term, which must be added to the molecular potential, and through restructuring of the Boltzmann factors for the initial state population. For a molecule in a state with rotational quantum number N, the potential is[21]

$$V(r) = V_0(r) + N(N+1)\hbar^2/2\mu R^2, \tag{4}$$

where V_0 is the potential for no rotation and μ is the reduced mass of the molecule. The vibrational wavefunction must be calculated for each rotational state, and Eq. (1) is replaced by

$$\sigma_{N''N'\epsilon'}(\lambda) = [\pi/(3\epsilon_0\hbar c g''\lambda)] \left| \int_0^\infty \psi_{N''\epsilon''}(r) R_e(r) \psi_{N'\epsilon'}(r)\, dr \right|^2. \tag{5}$$

If N'' is the initial state rotational quantum number, then transitions will occur to states in which the dissociating molecule has quantum numbers $N' = N'' \pm 1$, the two values of N' corresponding to slightly different final state potentials. An excellent approximation is obtained by assuming that $N' = N''$ for all transitions and then the total cross section is given by

$$\sigma_T(\lambda) = \left[\sum_{\epsilon''} \sum_{N''} (2N''+1)\, e^{-(G_{\epsilon''} + F_{N''\epsilon''})/kT} \sigma_{N''\epsilon''}(\lambda) \right] \Big/ \left[\sum_{\epsilon''} \sum_{N''} (2N''+1)\, e^{-(G_{\epsilon''} + F_{N''\epsilon''})/kT} \right], \tag{6}$$

where $F_{N''\epsilon''}$ and $G_{\epsilon''}$ are the initial state rotational and vibrational excitation energies, respectively, and $\sigma_{N''\epsilon''}$ is the cross section given by Eq. (5) with $N' = N''$.

The possibility that states other than $B^3\Sigma_u^-$ contribute to the absorption continuum in this region has been considered by several authors. Cartwright *et al.*[22] on the basis of electron energy-loss spectra, suggested that absorption to $^3\Pi_u$ and $^3\Pi_g$ states is significant near 143 and 166 nm, respectively. Measurements of the quantum yield for $O(^1D)$ production by photoabsorption[23] show no evidence of $^3\Pi$ continua in this region and calculations of the $^3\Pi_u$ continuum[24] indicate that the cross section is negligible for wavelengths longer than 140 nm. In this work, it has been assumed that absorption to $^3\pi$ states is insignificant, and Eq. (6) was used to calculate the temperature dependent cross section.

CALCULATIONS

Numerical solutions to the Schrödinger equation for the vibrational wavefunction were obtained using the Numerov integration method.[24,25] The potentials for no rotation were devised in the following way. For the ground state, an RKR potential was calculated using the spectroscopic constants of Creek and Nicholls.[27] Following the method of Jarmain,[28] the potential for the upper state was composed of three parts: for the lower part an RKR potential was calculated, and for the remaining repulsive and attractive parts, Morse potentials were used. Thus, the upper state potential in the energy region of the continuum was represented by a Morse potential,† the parameters of which were adjusted during the procedure to optimise the agreement between the calculated and measured quantities.

The procedure adopted in optimising the models for the upper state potential and the transition moment in the continuum was as follows. Initial calculations were made with Eq. (5), using an approximate model for the transition moment. The upper state potential curve was adjusted until the agreement between the measured and the calculated temperature dependence of the cross section was optimised. Then the transition moment was adjusted until agreement between the measured and calculated cross section at a particular temperature was optimised. Calculations made using widely different forms for the transition moment for given potential curves were found to produce very similar results for the temperature dependences of the cross section, but these results were very sensitive to changes in the potential curve used for the upper state. For this reason, determination of the upper state potential from the measured temperature dependence is possible. Because the new transition moment gave a calculated temperature dependence only slightly different from the previous result, repetition of the procedure yielded self-consistent results for the potential and transition moment in one or two cycles.

The results of these calculations are contained in Fig. 3, where the measured and calculated temperature dependence for the temperature interval 300–575K are shown. The solid curve in Fig. 4 is the final transition moment and some points on the potential that was used are listed in Table 2.

†The actual potential used in the calculations included a plateau due to non-crossing of potential curves.[29,30] Its effects on the temperature dependence of the cross-section in the wavelength region considered in the present paper are small. The shorter wavelength region will be discussed in a future paper.

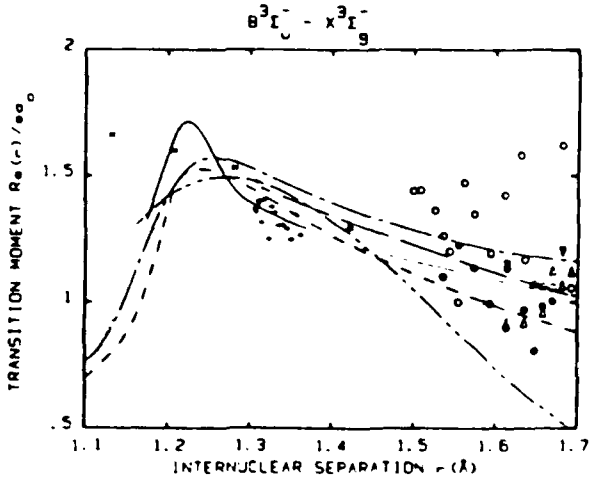

Fig. 4. Electronic transition moment for the Schumann-Runge transition in O_2. — · — · — present model, – – — – – —, model of Allison *et al.*[26] — · · — · · —, experimental curve of Kuz'menko *et al.*[31] Points obtained from experimental band measurements were derived from the data of Gies *et al.* (+), Treanor and Wurster[32] (○), Krindach *et al.*[33] (●), Keck *et al.*[27] (△), Cooper[34] (▽), and Losev *et al.*[35] (▲). *Ab initio* calculations — — —, Buenker *et al.*;[36] ×, Julienne *et al.*;[37] — · — · —, Yoshimine *et al.*[38]

Table 2. Some points on the repulsive part of the potential curve for the $B^3\Sigma_u^-$ state of O_2 with no rotation that were used in the calculations. The potentials are given relative to the value at the equilibrium separation r_e

r, Å	$V_o(r) - V_o(r_e)$, eV
1.050	3.682
1.100	3.175
1.150	2.956
1.175	2.905
1.185	2.902
1.190	2.892
1.195	2.786
1.200	2.688
1.225	2.238
1.250	1.850
1.300	1.232
1.350	0.773
1.400	0.455

DISCUSSION

Ab initio calculations of the transition moment have been made by Buenker *et al.*,[29] Yoshimine *et al.*,[30] and Julienne *et al.*,[31] however, the only previously reported determinations with which these results can be compared are those derived from oscillator-strength measurements in the band system. The transition moment is related to the band oscillator strength $f_{v'v''}$ by[19]

$$f_{v'v''} = [8\pi^2 mc/(3he^2 g''\lambda)] \left| \int_0^\infty \psi_{v'} R_e(r) \psi_{v''} \, dr \right|^2. \tag{10}$$

Approximate values for the transition moment can be obtained from experimental measurements of band oscillator strengths through the r-centroid approximation.[19] The points shown in Fig. 4 were obtained from measurements of oscillator strengths in the Schumann-Runge bands and Franck–Condon factors that were computed using the potential curves adopted in this work. The possibility that a significant error may have been introduced through the use of the r-centroid approximation was checked by making a calculation for the (v'–0) bands using Eq. (10) with an extended model for the transition moment it was found that the error introduced by the r-centroid approximation is very small (<2%). The reason for the accuracy of the r-centroid approximation in this case is that the integrand in Eq. (10) corresponds to the overlapping exponential tails of the vibrational wavefunctions and has a significant value over only a small range of r. In other cases, the criterion $\overline{r^2}/\overline{r}^2 \approx 1$ was used as an indication that the error in the r-centroid approximation was small.[32] The scatter in the points shown in Fig. 4 is therefore a result of experimental error.

The effects of rotation on the calculation of the cross section are of two kinds. One is due to the rotational dependence of $\sigma_{N'v'}$, and this leads to temperature effects in the cross section which are significant compared to the measured temperature dependence. The variation of the curves for $\sigma_{N'0}$ with rotational number have been discussed previously.[33] This effect means that calculations such as those of Allison *et al.*,[20] which omit rotation, are inadequate for analysis of the temperature dependence of the absorption cross section. This is made clear by the curve in Fig. 3, which shows the result of calculating the temperature dependence of the cross section without including the rotational structure of the molecule.

The other effect is a redistribution of the population among vibrational states compared to that calculated in the absence of rotation. This is a very small effect because there is very little variation of the rotational constant with v'', so that

$$\sum_{N''} (2N'' + 1) e^{-F_{N''v''}/kT},$$

which appears in Eq. (6) is, to a good approximation, independent of v''.

Calculations of the total cross section as a function of temperature can be made at any

wavelength in the range 140–175 nm using Eq (6) with the potential of Table 2 and the transition moment shown in Fig. 4. Examples of this calculation for wavelengths of 149 and 165 nm are shown in Fig. 2. The positive temperature coefficient evident at temperatures less than 300K in both curves is a purely rotational effect. At higher temperatures, the vibrational effects become dominant.

Initial calculations of the temperature dependence of the cross section indicated that the interface between the repulsive part of the Morse potential and the bound part of the RKR potential should be made at the energy of the $v' = 14$ state. Any discontinuity in slope was removed by smoothing and the outer part of the curve recalculated by a modified RKR method. The resulting potential has bound state eigenvalues that agree with spectroscopic measurements to within 1 cm^{-1}. Optimisation of the parameters of the Morse extension led to the curve for the calculated temperature dependence of the cross section that is shown in Fig. 3 and the solid part of the curve for the transition moment shown in Fig. 4 for $r < 1.3$ Å. It can be seen that there is a small discrepancy between the calculated and experimental temperature coefficients in the region from 168 to 174 nm.

This discrepancy could be eliminated by using a non-Morse extension to the potential. The result was a potential curve for which the second derivative was not monotonic. Furthermore, the Franck–Condon densities calculated with this potential had structure that led to compensating structure in the transition moment to give the smoothly varying total cross section.

If it is assumed that the transition moment varies slowly without such structure, then the smooth form of the total cross section must indicate that both the transition moment and the Franck–Condon density are without structure, and the second derivative of the potential should be monotonic. With this constraint on the form of the potential, the optimum Morse extension to the potential produced a better result than any other form investigated and it was concluded that the curves shown in Figs. 3 and 4 represent the best interpretation of the data. The small discrepancies in Fig. 3 may be due to an unrecognised systematic error in the measurements.

The calculation of the cross section at any wavelength is sensitive to the transition moment over a small range of internuclear separation. For the wavelength interval 140–175 nm, the overlap of initial and final state wavefunctions lies mainly in the range of internuclear separation from 1.18 to 1.3 Å, corresponding to the solid part of the model for the transition moment shown in Fig. 4. Because there is some overlap outside this range, the model was extended to 1.1 Å in the calculations, but the comparison between measured and calculated cross sections for wavelengths greater than 140 nm is not very sensitive to this part of the curve.

The transition moment determined from the continuum measurements is consistent with the values for internuclear separation close to 1.33 Å obtained from measurements of the (v'–0) band oscillator strengths. The points shown were obtained from the data of Gies *et al.*[18] The model transition moment was extended to 1.7 Å by reference to measurements of the oscillator strengths for bands corresponding to $v'' \neq 0$. These measurements were made at high effective temperatures using a shock tube, and there is considerable scatter in the results. The line shown in Fig. 4 was drawn by giving greatest weight to the measurements of Krindach *et al.*[34] The *ab initio* calculations Buenker *et al.*,[29] Yoshimine *et al.*,[30] and Julienne *et al.*,[31] are in good agreement with the model for inter-nuclear distances greater than 1.3 Å. The curve adopted by Kuz'menko *et al.*[35] on the basis of band-strength measurements is also shown in Fig. 4.

The small increase in the temperature coefficient of the cross-section that is apparent in Fig. 3 at wavelengths close to 140 nm is continued in data obtained at shorter wavelengths. It is necessary to introduce a plateau in the potential to reproduce this feature in the calculated temperature coefficient. A decrease in the derived transition moment for internuclear separations less than 1.22 Å follows from this form of the potential. This is consistent with *ab initio* calculations of Buenker *et al.*[29] and Yoshimine *et al.*[30] The decrease corresponds in the *ab initio* calculations to a change in character of the upper state from valence to Rydberg type because of an avoided potential crossing. The calculations of Julienne *et al.*[31] which included only the valence state, do not show this feature.

In conclusion, we have shown that accurate measurements of continuum photoabsorption cross sections at two widely separated temperatures provided adequate information to yield unambiguous values for the continuum part of the upper state potential and the dipole moment for the transition.

Acknowledgements—This work was supported by grants from the Australian Research Grants Scheme and the U.S. Air Force Geophysics Laboratory. The authors wish to thank F. A. Smith for assistance in obtaining the experimental data.

REFERENCES

1. R. Landenburg, C. C. van Voorhis, and J. C. Boyce, *Phys. Rev.* **40**, 1018 (1932).
2. E. G. Schneider, *J. Chem. Phys.* **5**, 106 (1937).
3. R. W. Blackburn and D. W. O. Heddle, *Proc. Roy. Soc. (Lond).* **A220**, 61 (1953).
4. K. Watanabe, E. C. Y. Inn, and M. Zelikoff, *J. Chem. Phys.* **21**, 1026 (1953).
5. E. T. Bryan, T. A. Chubb, and H. Friedman, *Phys. Rev.* **98**, 1594 (1955).
6. K. Watanabe and F. F. Marmo, *J. Chem. Phys.* **25**, 965 (1956).
7. K. Watanabe, *Advances in Geophysics* **5**, 157 (1958).
8. J. S. Evans and C. J. Schexnayder, "An Investigation of the Effect of High Temperature on the Schumann-Runge Ultraviolet Absorption Continuum of Oxygen". *Tech. Rep.* R-92. Langley Research Centre, Langley Field, Virginia (1961).
9. P. H. Metzger and G. R. Cook, *JQSRT* **4**, 107 (1964).
10. R. E. Huffman, Y. Tanaka, and J. C. Larrabee, *Disc. Faraday Soc.* **37**, 159 (1964).
11. R. D. Hudson, V. L. Carter, and J. A. Stein, *J. Geophys. Res.* **71**, 2295 (1966).
12. A. J. Blake, J. H. Carver, and G. N. Haddad, *JQSRT* **6**, 451 (1966).
13. R. Goldstein and F. N. Mastrup, *J. Opt. Soc. Am.* **56**, 765 (1966).
14. R. D. Hudson, *Rev. Geophys. Space Phys.* **9**, 305 (1971).
15. J. H. Carver, L. A. Davis, B. H. Horton, and M. Ilyas, *J. Geophys. Res.* **83**, 4377 (1978).
16. L. H. Weeks, *J. Geophys. Res.* **80**, 3661 (1975).
17. J. L. Lean and A. J. Blake, *J. Geophys. Res.* **86**, 211 (1981).
18. H. P. F. Gies, S. T. Gibson, D. G. McCoy, A. J. Blake, and B. R. Lewis, *JQSRT* **26**, 469 (1981).
19. W. R. Jarmain and R. W. Nicholls, *Proc. Phys. Soc.* **84**, 417 (1964).
20. A. C. Allison, A. Dalgarno, and N. W. Pasachoff, *Planet Space Sci.* **19**, 1463 (1971).
21. G. Herzberg, *Spectra of Diatomic Molecules*. Van Nostrand, New York (1950).
22. D. C. Cartwright, N. A. Fiamengo, W. Williams, and S. Trajmar, *J. Phys. B.* **9**, L419 (1976).
23. L. C. Lee, T. G. Slanger, G. Black, and R. L. Sharpless, *J. Chem. Phys.* **67**, 5602 (1977).
24. A. C. Allison, S. L. Guberman, and A. Dalgarno, private communication (1981); S. L. Guberman and A. Dalgarno, *J. Geophys. Res.* **84**, 4437 (1979).
25. J. K. Cashion, *J. Chem. Phys.* **39**, 1872 (1963).
26. A. C. Allison, *Comp. Phys. Com.* **1**, 21 (1969).
27. D. M. Creek and R. W. Nicholls, *Proc. Roy. Soc. Lond* **a341**, 517 (1975).
28. W. R. Jarmain, *JQSRT* **11**, 421 (1971).
29. R. J. Buenker, S. D. Peyerimhoff, and M. Peric, *Chem. Phys. Lett.* **42**, 383 (1976).
30. M. Yoshimine, K. Tanaka, H. Tatewaki, S. Obara, F. Sasaki, and K. Ohno, *J. Chem. Phys.* **64**, 2254 (1976).
31. P. S. Julienne, D. Neumann, and M. Krauss, *J. Chem. Phys.* **64**, 2990 (1976).
32. J. Drake and R. W. Nicholls, *Chem. Phys. Lett.* **3**, 457 (1969).
33. H. P. F. Gies, S. T. Gibson, A. J. Blake, and D. G. McCoy, *J. Geophys. Res. J. Geophys. Res.* **87**, 8307 (1982).
34. N. I. Krindach, N. N. Sobolev, and L. N. Tunitskii, *Opt. Spektrosk (USSR)* **15**, 298 (1963).
35. N. E. Kuz'menko, L. A. Kusnetsova, A. P. Monyakin, and Y. Y. Kuzyakov, *JQSRT* **24**, 29 (1980).
36. C. E. Treanor and W. H. Wurster, *J. Chem. Phys.* **32**, 758 (1960).
37. J. C. Keck, J. C. Camm, B. Kivel, and T. Wentink, *Ann. Phys.* **7**, 1 (1959).
38. D. M. Cooper, *JQSRT* **17**, 543 (1977).
39. S. A. Losev and N. A. Generalov, *Optika i spectrospija* Vol. II, p. 15, AN USSR, Moscow (1963).

JOURNAL OF GEOPHYSICAL RESEARCH, VOL. 86, NO. A1, PAGES 211-214, JANUARY 1, 1981

THE EFFECT OF TEMPERATURE ON THERMOSPHERIC MOLECULAR OXYGEN ABSORPTION IN THE SCHUMANN-RUNGE CONTINUUM

J. L. Lean and A. J. Blake

Department of Physics, University of Adelaide
ADELAIDE, AUSTRALIA 5001

Abstract. Previous determinations of molecular oxygen number densities in the lower thermosphere by ultraviolet extinction in the Schumann-Runge continuum have used absorption cross sections measured at room temperature. Recent laboratory measurements of the temperature dependence of the molecular oxygen absorption cross section in this wavelength region allow a reassessment of the previous atmospheric data. The new cross sections have been used to reanalyze data from a spectrometer flown on an Aerobee rocket from Woomera, Australia. The densities obtained are smaller by as much as 20% than those obtained from the previous analysis, in better agreement with the results of broad band ion chambers flown at the same time that were relatively insensitive to temperature.

Introduction

The Schumann-Runge absorption continuum of molecular oxygen extends over the wavelength region 140 to 175 nm. Solar radiation at these wavelengths is absorbed by the atmosphere between altitudes of 100 and 150 km, and this is the primary source of O_2 photodissociation in the lower thermosphere. Absorption spectroscopy techniques for O_2 density determination are particularly appropriate for solar radiation of these wavelengths, since here the absorption cross section of O_2 is large and the radiation is primarily absorbed by O_2.

In the study of atmospheric photochemistry [Roble and Dickinson, 1973; Breig, 1973; Oran and Strobel, 1976; Mayr and Harris, 1977], as well as for application of absorption as a tool for quantitative composition analysis [Ackerman et al., 1974], it is necessary to know in detail how the solar flux is absorbed by thermospheric oxygen. This involves the accurate determination of O_2 absorption cross sections in the laboratory under conditions representative of the atmospheric region where the absorption occurs. In particular, in the region from 100 to 150 km, the thermospheric temperature may vary over the range 200K to 600K, and this influences the O_2 absorption.

Although the temperature dependence of molecular oxygen absorption in the Schumann-Runge continuum has been calculated theoretically [Evans and Schexnayder, 1961; Jarmain and Nicolls, 1964; Allison et al., 1971; Julienne et al., 1976] there have been only two previous experimental measurements [Evans and Schexnayder, 1961; Hudson et al., 1966], and the results are not well formulated for use in aeronomic calculations.

Paper number 80A1133.
0148-0227/81/080A-1133$01.00

Temperature Dependence of Molecular Oxygen Absorption in the Schumann-Runge Continuum

The Schumann-Runge continuum corresponds to transitions from discrete vibrational levels of the $X^3\Sigma_g^-$ state of O_2 to the energy region above the dissociation limit of the $B^3\Sigma_u^-$ state. At room temperature, absorption is mainly from the lowest vibrational level of the ground state $v'' = 0$, but at higher temperatures, transitions from excited vibration states must be considered. This can be done, as suggested by Allison et al., [1971], by weighting the cross section $\sigma_{v''}$ for absorption by molecules in each vibration state v'' according to its population, so that at temperature T and wavelength λ, the absorption cross section can be expressed analytically as

$$\sigma(T,\lambda) = \frac{\Sigma_{v''}\sigma_{v''}(\lambda)\exp(-G_{v''}hc/kT)}{\Sigma_{v''}\exp(-G_{v''}hc/kT)} \quad (1)$$

where $G_{v''}$ is the vibrational term value [Herzberg, 1950]. Using the first two terms of the summation in (1), the Schumann-Runge continuum cross section is

$$\sigma(T,\lambda) = \frac{\sigma_0(\lambda) + \sigma_1(\lambda)\exp(-2239.29/T)}{1 + \exp(-2239.29/T)} \quad (2)$$

The value of $\sigma_0(\lambda)$ is given to a good approximation by the experimental cross section at room temperature, and this has been measured by Watanabe et al., [1953], Blake et al., [1966], Hudson et al., [1966], and most recently at the University of Adelaide, with a 6-m monochromator [Blake et al., 1980]. These results are compared in Figure 1 and an average cross section is also indicated.

Measurements of $\sigma(T,\lambda)$ for temperatures in the range 300K to 600K have been made by Hudson et al., [1966] and the University of Adelaide. Both sets of results are plotted in Figure 2, and for comparison, selected average room temperature cross sections from Figure 1 have been included. Values of $\sigma_1(\lambda)$ were obtained from the University of Adelaide measurements at 570K by using (2) with the average room temperature cross sections for $\sigma_0(\lambda)$ and the $\sigma_1(\lambda)$ derived in this way. The results for selected wavelengths are given in Figure 3.

Rocket Measurement of Absorption in the Schumann-Runge Continuum

Solar flux in the wavelength region of the Schumann-Runge continuum was measured at different

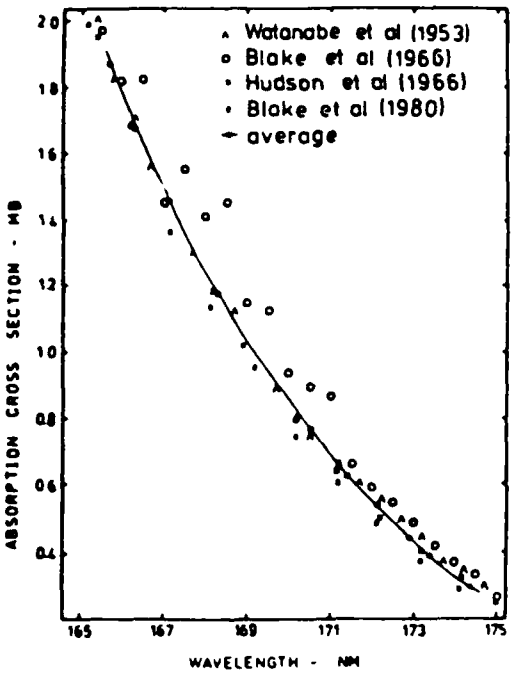

Fig. 1. Room temperature measurements of the absorption cross section of molecular oxygen.

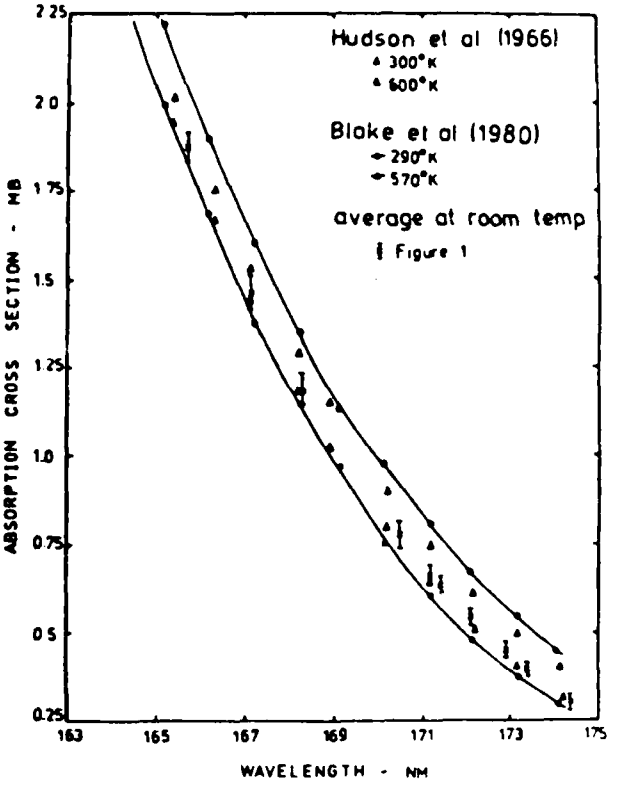

Fig. 2. Measurements of the temperature dependence of the molecular oxygen absorption cross section.

altitudes with a scanning 1m Ebert Fastie spectrometer, flown on an Aerobee vehicle at a time when the solar zenith was 85°, as part of a composite payload for investigating the early morning ionosphere. Initial analysis of the absorption profiles for O_2 density derivation incorporated the room temperature cross section measurements of Blake [Blake et al., 1966] and has been reported previously [Bibbo et al., 1978]. The data has been reanalyzed with the average room temperature cross section and by using the temperature dependent absorption cross section, in order to quantify the importance of the temperature dependence on density determination using Schumann-Runge continuum wavelengths.

Monochromatic absorption profiles from ten narrow wavelength intervals between 165 and 175 nm were used to calculate O_2 densities according to

$$n(h) = \frac{1}{\sigma(\lambda)\ F(h)\ I(\lambda, h)} \cdot \frac{dI}{dh}\ (\lambda, h)$$

where $F(h)$ is the optical depth factor [Weeks and Smith, 1968], $\sigma(\lambda)$ is the absorption cross section and $I(\lambda\ h)$ is the detector signal arising from solar radiation at wavelength λ that has penetrated to height h.

The most accurate densities derive from that part of each absorption curve in the region about the altitude at which the rate of attenuation is a maximum, and this is different for each wavelength. At height h an average oxygen density was calculated by weighting the individual densities according to $(dI(\lambda, h)/dh)_i^{-1}$ and the mean weighted sample standard deviation was used to estimate the uncertainty in this average value.

To incorporate temperature dependent absorption cross sections in the data analysis, it

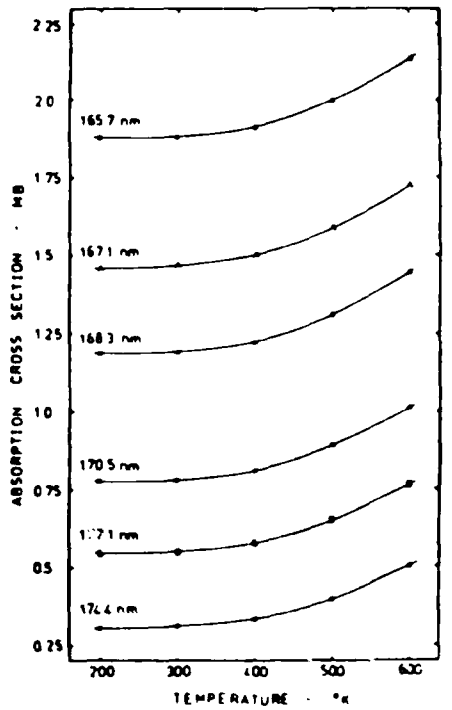

Fig. 3. Semi-empirical model of the temperature dependence of the molecular oxygen absorption cross section.

is necessary to assume a temperature profile for the lower thermosphere. Jacchia's [Jacchia, 1977] thermospheric model was evaluated for the temperature profile at the time of the Aerobee launch. This temperature profile is compared (Figure 4) with that of the U.S. Standard Atmosphere, (1976) for more typical thermospheric conditions.

Molecular Oxygen Densities

Oxygen densities were extracted from the absorption curves by using the average room temperature cross sections of Figure 1, and also the temperature dependent cross sections calculated by using temperature profiles (a) and (b) of Figure 4 in (2). These results are shown in Figure 5, together with the measurement made by the ion chambers and the oxygen densities derived from Jacchia's thermospheric composition model.

In general, inclusion of the temperature dependence of the cross section leads to smaller numerical values for the oxygen densities. At 125 km the thermosphere is approximately at room temperature, and it is above this altitude that the temperature dependence is observed to become important. By 145 km the temperature, according to profile (b), is 536K and the room temperature cross sections yield densities which are 11% higher than those derived from temperature dependent cross sections. At 165 km the densities are overestimated by 23% if the temperature effect is not included.

The importance of using the temperature dependent absorption cross sections in these calculations is substantiated by an observed decrease in the weighted mean standard deviation of the densities obtained by using absorption at different wavelengths when the temperature effect

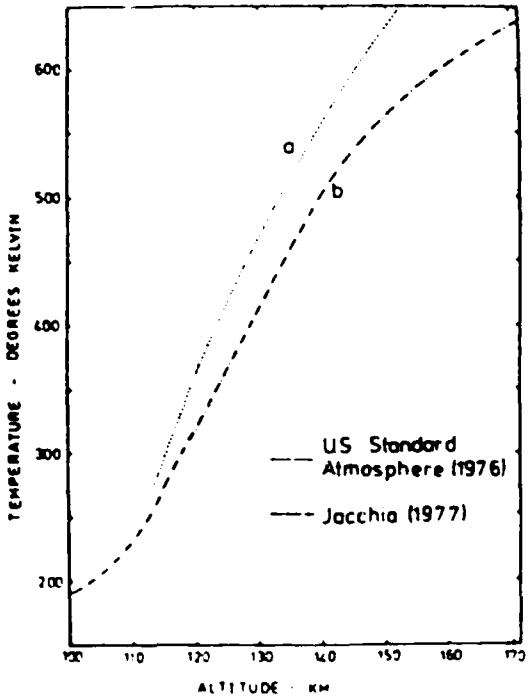

Fig. 4. Temperature profiles for the lower thermosphere.

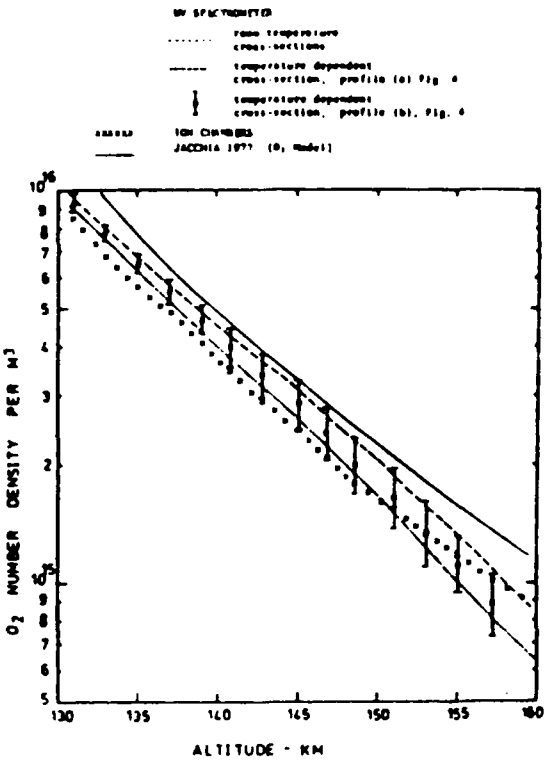

Fig. 5. Molecular oxygen number densities.

is included. This implies that the densities predicted individually by each of the ten absorption curves are now in better agreement with each other because the temperature dependence of the cross section varies with wavelength.

It can be seen from Figure 5 that the oxygen densities obtained from the absorption data are sensitive to the differences between the temperature profiles shown in Figure 4. At an altitude of 145 km the temperature from profile (a) gives densities which are 5% less than that obtained using profile (b), while at 165 km the difference has increased to 11%. The Aerobee was launched during a period of low solar activity

$$(F_{10.7} = 82 \times 10^{-22} Wm^{-2}Hz,\ K_p = 1^-)$$

at a time (0636 hours local time) when the diurnal variation of the thermospheric temperature was near its minimum. These conditions are reflected in the lower temperatures of profile (b) compared with profile (a), which represents more typical conditions.

In Figure 5, the O_2 densities derived from the temperature dependent analysis are compared with the average measurements of two types of broad-band ion chambers (QT : 156-165 nm, SX : 142.5-149 nm) flown on the Aerobee. Investigation of the temperature effect on the QT results indicated 3% decrease in the density at 145 km (Davis, private communication, 1980). Since the temperature coefficient for the cross section at the SX chamber wavelengths is small and negative [Blake et al., 1980], the average density shown in Figure 5 is relatively insensitive to temperature. At 145 km the UV spectrometer results are 13% higher than the ion chamber densities. Since the associated

uncertainty for the spectrometer results at this altitude is ± 15%, when the error of the ion chamber results is applied the results from these two independent techniques indicate substantial agreement. However, this cannot be said of the densities derived by using room temperature cross sections, since at 145 km they are 29% higher than the ion chamber results.

It must be concluded that the temperature dependence of the molecular oxygen absorption cross section in the Schumann-Runge continuum should not be neglected in evaluation of atmospheric absorption and that it is important to choose the most appropriate temperature profile.

Acknowledgments. This work has been supported by the Australian Research Grants Committee.

The editor thanks E. Oran for his assistance in evaluating this brief report.

References

Ackerman, M., P. Simon, U. von Zahn and U. Laux, Simultaneous upper air composition measurements by means of UV monochromators and mass spectrometers, J. Geophys. Res., 79, 4757, 1974.

Allison, A.C., A. Dalgarno, and N. W. Passchoff, Absorption by vibrationally excited molecular oxygen in the Schumann-Runge continuum, Planet. Space Sci., 19, 1463, 1971.

Bibbo, G., J.H. Carver, L.A. Davis, B.H. Horton and J.L. Lean, UV extinction and mass spectrometer rocket measurements of atmospheric composition over Woomera, Space Res., 19, 225, 1978.

Blake, A.J., J.H. Carver, and G.N. Haddad, Photo-absorption cross sections of molecular oxygen between 1250Å and 2350Å, J. Quant. Spectrosc. Radiat. Transfer, 6, 451, 1966.

Blake. A.J., D.G. McCoy, H.P.F. Gies, and S.T. Gibson, Photoabsorption in molecular oxygen, Interim Sci. Rep.,15 Sept. 1978-30 Nov.1979, Air Force Geophys. Lab.,Hanscom AFB, MA,1980.

Breig, E.L., Aeronomic consequences of solar flux variations between 2000 and 1325 Angstroms, J. Geophys. Res., 78, 5718, 1973.

Evans. J.S., and C.H. Schexnayder, Jr., An investigation of the effect of high temperature on the Schumann-Runge ultraviolet absorption continuum of oxygen, NASA Tech. Rep. R-92, 1961.

Herzberg, G. Spectra of Diatomic Molecules, Van Nostrand Reinhold, New York, 1950.

Hudson, R.D., V.L. Carter, and J.A. Stein, An investigation of the effect of temperature on the Schumann-Runge absorption continuum of oxygen, 1580-1950Å, J. Geophys. Res., 71, 2295, 1966.

Jacchia, L.G.,Thermospheric temperature, density and composition: New models, Spec. Rep. 375, Smithson Astrophys. Observ., Cambridge, Mass., 1977.

Jarmain, W.R. and R.W. Nicholls, A theoretical study of the $O_2X^3\Sigma_g^- - B^3\Sigma_u^-$ photodissociation continuum, Proc. Phys. Soc. London, 84, 417, 1964.

Julienne, P.S., D. Neumann and M. Krauss, Transition moments for the $B^3\Sigma_u^- - X^3\Sigma_g^-$ and $^1\Pi_u - X^3\Sigma_g^-$ transitions in O_2, J. Chem. Phys., 64, 2990, 1976.

Mayr, H.G., and I. Harris, Annual variation in temperature and composition of the thermosphere and upper mesosphere, Space Res. 17, 293, 1977.

Oran, E.S., and D.F. Strobel, Photochemically induced departures of [O] and [O_2] from diffusive equilibrium distributions, J. Geophys. Res., 81, 257, 1976.

Roble, R.G., and R.E. Dickinson, Is there enough solar extreme ultraviolet radiation to maintain the global mean thermospheric temperature ?, J. Geophys. Res., 78, 249, 1973.

Watanabe, K., E.C.Y. Inn, and M. Zelikoff, Absorption coefficients of oxygen in the vacuum ultraviolet, J. Chem. Phys., 21, 1026, 1953.

Weeks, L.H., and L.G. Smith, Molecular oxygen concentrations in the upper atmosphere by absorption spectroscopy, J. Geophys. Res., 73, 4835, 1968.

(Received February 28, 1980;
accepted July 21, 1980.)

JOURNAL OF GEOPHYSICAL RESEARCH, VOL. 87, NO. A10, PAGES 8307-8310, OCTOBER 1, 1982

THE SCHUMANN-RUNGE CONTINUUM OF OXYGEN AT WAVELENGTHS GREATER THAN 175 NM

H. P. F. Gies,[1] S. T. Gibson, A. J. Blake and D. G. McCoy

Department of Physics, University of Adelaide, Adelaide,

South Australia 5001, Australia

Abstract. A highly temperature dependent continuum corresponding to absorption by thermally excited molecules underlies the higher bands of the Schumann-Runge system of oxygen. This continuum has been experimentally determined at 18 wavelengths in the range 175 nm to 179 nm, and at temperatures of 90°K and 294°K. Calculations of the continuum cross-section made by solving the Schrödinger equation for the molecular potentials provide good agreement with the measured values. The continuum cross-section has been calculated at a range of temperatures for use in studies of the atmospheric absorption of solar radiation.

Introduction

For oxygen molecules with rotational or vibrational excitation the threshold for absorption in the Schumann-Runge continuum is at a greater wavelength than the limit of the band system at 175 nm. The strength of the continuum that underlies the higher bands depends on the population of these excited states in the absorbing gas and is therefore highly temperature dependent. Because absorption of solar radiation in the region of the Schumann-Runge bands is an important source of oxygen atoms in the atmosphere, there is a need to model accurately the absorption process. For temperatures that occur in the lower thermosphere, this continuum makes a significant contribution to the absorption cross-section in the region of bands higher than (15-0) [Blake, 1979] and should be taken into account when calculating the atmospheric transmission.

Measurements of the continuum cross-section in this region have been reported by Hudson et al. [1966] and Hudson and Mahle [1972]. Models of the continuum for use in the calculation of atmospheric transmission have been proposed by Hudson and Mahle [1972] and Blake [1979]. In the present paper values of the Schumann-Runge continuum cross-section are obtained from measurements of the total cross-section at absorption minima. The continuum cross-section is also obtained by making detailed calculations of the continuum transition strength. These calculations provide a suitable model for use in atmospheric absorption studies.

Experimental Measurements

At wavelengths greater than the limit of the band system the continuum cross-section cannot be measured directly because the wings of the predissociated lines overlap. However, there are some absorption minima where the contribution from absorption lines is relatively small and the continuum cross-section can be determined by measuring the total cross-section at the wavelength of the absorption minimum and subtracting the contribution from the neighbouring absorption lines. In this work that contribution was calculated by using measured values for the oscillator strengths and predissociation widths for the absorption lines.

Measurements of total absorption were made in the region of 18 absorption minima in the wavelength region 175 nm to 179 nm. A scan through each minimum was made by using a 6.7-m monochromator at a resolution of 0.006 nm and a 1-cm absorption cell that could be cooled with cryogenic liquids. Details of the apparatus and the experimental method have been described previously [Gies et al., 1981]. Absorption measurements were made at temperatures of 90°K and 294°K.

The band system contribution to the cross-section at each wavelength was calculated by computing the Voigt profile for each absorption line with center within 100 cm^{-1} of the absorption minimum. Oscillator strengths and predissociation widths for the lines were obtained from measurements that have been reported separately [Gies et al., 1981]. The computed transmission spectrum in the region of the absorption minimum was convoluted with the instrumental profile, and comparison of this computed absorption profile with the measured profile enabled the continuum cross-section to be determined. Table 1 shows the calculated band system contribution to the cross-section at the wavelengths of the absorption minima, and the continuum values obtained by subtracting these from the measured total cross-section. The continuum cross-section values are shown in Figure 1.

The errors quoted for values of the continuum cross-section were obtained by combining the experimental error in determining the total absorption cross-section with the error in calculating the contribution from absorption lines. Total cross-sections were measured with an error of about 3% arising from factors such as

[1]Now at Australian Radiation Laboratory, Yallambie, Victoria 3085, Australia.

Paper number 2A0936.
0148-0227/82/002A-0936$02.00

Table 1. Calculated Cross-Section for the Band System and derived Continuum Cross-Section at Temperatures of 90°K and 294°K.

	T = 90°K		T = 294°K	
Wavelength	Bands	Continuum	Bands	Continuum
175.48	6.5	23.0 ± 1.9	3.6	113.5 ± 2.1
175.55	-	-	3.8	119.3 ± 8.0
175.63	9.8	34.2 ± 0.9	4.9	111.5 ± 4.6
175.71	7.4	18.4 ± 5.6	5.1	76.6 ± 2.1
175.83	4.5	14.2 ± 1.1	6.3	55.7 ± 2.4
175.96	29.9	6.0 ± 2.6	15.6	39.6 ± 2.6
176.05	8.6	1.3 ± 1.7	7.2	46.8 ± 2.2
176.16	2.3	7.5 ± 1.2	2.8	36.1 ± 1.4
176.23	4.8	6.8 ± 1.1	7.7	37.1 ± 1.4
176.27	2.6	1.5 ± 2.4	3.7	37.4 ± 1.4
176.53	-	-	11.7	27.8 ± 1.4
176.56	-	-	7.3	27.5 ± 2.4
176.61	4.6	5.1 ± 1.8	6.1	30.2 ± 3.5
176.80	-	-	2.6	17.7 ± 1.3
177.02	4.3	5.0 ± 1.9	10.9	25.5 ± 3.3
178.92	-	-	0.9	3.7 ± 1.2
178.95	-	-	1.0	3.8 ± 2.0
179.02	-	-	0.7	3.8 ± 1.2

All values are in units of 10^{-21} cm^2.

gas pressure, gas temperature, cell length and beam intensity. Errors in computing the line wings arise from uncertainty in the values of the line position, line strength, and predissociation width for those lines that make a significant contribution.

Calculation of Continuum Cross-Sections

An expression for the continuum absorption cross-section for molcules in a particular vibrational level has been given by Jarmain and Nicholls [1964]. With the inclusion of rotation, the equation for the absorption cross-section of oxygen molecules initially in a state characterised by the rotational quantum number N^- and vibrational quantum number v^- becomes

$$\sigma_{N^-v^-}(\lambda) = [\pi/(3\epsilon_0 hc g^- \lambda)] \left| \int_0^\infty \Psi_{N^-v^-}(r)\, R_e(r)\, \Psi_{N^-\lambda}(r) dr \right|^2 \quad (1)$$

where $g^- = (2-\delta_{0\Lambda^-})(2S+1)$ is the statistical weight of the initial state, $\Psi_{N^-v^-}$ and $\Psi_{N^-\lambda}$ are the normalized initial and final state vibrational wave functions for the rotating molecule, R_e is the electronic transition moment, and r is the internuclear distance.

Vibrational wavefunctions were found by solving the Schrödinger equation by using the potential for a rotating molecule given by [Herzberg, 1950]

$$V(r) = V_o(r) + N^-(N^-+1)\,\hbar^2/2\mu r^2 \quad (2)$$

where V_o is the potential for no rotation and μ is the reduced mass of the molecule.

In making calculations of $\sigma_{N^-v^-}$, the potential V_o for the $X^3\Sigma_g^-$ and $B^3\Sigma_u^-$ states of oxygen and the transition were those determined in a study of the Schumann-Runge continuum at wavelengths less than 174 nm (S.T. Gibson et al., unpublished manuscript, 1982). These curves reproduce the Schumann-Runge continuum cross-

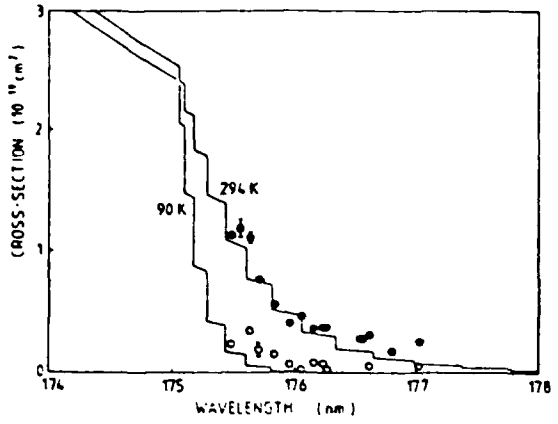

Fig. 1. Schumann-Runge continuum cross-section. Values derived from experimental measurements: 294°K,(solid circles), and 90°K (open circles). The solid lines are the model cross-section at temperatures of 90°K and 294°K.

section and its temperature dependence at wavelengths in the range 140 nm to 175 nm. Some examples of $\sigma_{N''v''}(\lambda)$ for $v''=0$, shown in Figure 2, illustrate the change in the form of these curves with N''.

The total continuum cross-section at any wavelength λ and temperature T was computed by summing over all initial states that contribute to the continuum, weighting each cross-section by the population of the initial state in the absorbing gas using the equation

$$\sigma_T(\lambda) = \frac{\sum_{v''=0}^{2} \sum_{N''} (2N''+1)\, \sigma_{N'',v''}(\lambda) \exp[-E_{N'',v''}/kT]}{\sum_{v''=0}^{2} \sum_{N''} (2N''+1) \exp[-E_{N'',v''}/kt]} \qquad (3)$$

where $E_{N'',v''}$ is the energy of the initial state of the molecule and N'' is summed over all values that give a threshold for continuous absorption at a wavelength greater than λ. Cross-sections corresponding to temperatures of 90°K and 294°K are shown in Figure 1 where they can be compared with the values obtained from measurement. The model was used to calculate the cross-section for a range of temperatures between 100°K and 600°K. These curves are shown in Figure 3.

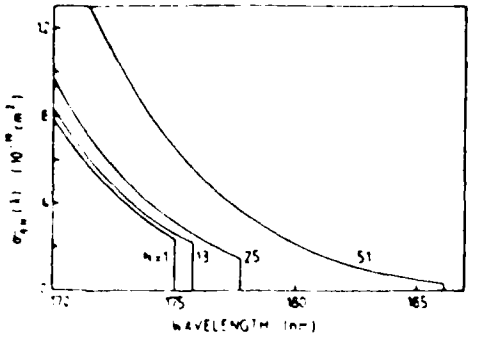

Fig. 2. Calculated Schumann-Runge continuum cross-sections for molecules in the initial states with $v''=0$ and $N''=1$, 13, 25 and 51.

Discussion

The model cross-section is a detailed one, and comparison with measurements provides a test of the method used in the calculation and the molecular parameters on which it is based. Thresholds corresponding to each initial state from which significant absorptions occurs can be seen in the curves of Figures 1 and 3. For large N'' these thresholds occur at slightly shorter wavelengths than the values given by the dissociation limit for the $B^3\Sigma_u^-$ state because of the effect of the centrifugal barrier in the potential for a rotating molecule. At some thresholds the calculations indicate resonance effects in the cross-section due to the potential barrier, but it is unlikely that these effects could be observed, and they are not shown in the figures. The threshold cross-section is also seen to decrease with increasing N''. This is because the intergrand of (1) corresponds to the overlap of decaying 'tails' of vibrational wavefunctions, and the effect of the rotational term in (2) is to modify the potentials so that this overlap is reduced. It is partly for this reason that the present cross-section departs from the exponential forms assumed by Hudson and Mahle [1972].

Figure 1 shows that the computed cross-section is in general agreement with the values deduced from measurements, although the number of measurements is not enough to demonstrate the step-like structure. In some cases there are significant discrepancies between the model and the points derived from experimental data. These discrepancies arise from an error in the calculated contribution of absorptions lines to the measured total cross-section when weak lines that are perturbed or unaccounted for occur near the absorption minimum being measured [Gies et al., 1981]. It should be expected that these discrepancies would be most significant at low temperatures, probably accounting for the points at 90°K being consistently higher than the model

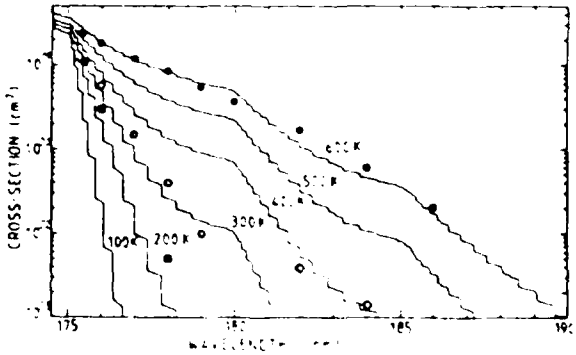

Fig. 3. Model Schumann-Runge cross-sections for temperatures between 100°K and 600°K. Also shown are measurements of Hudson et al. (600°K (solid circles), and 300°K (open circles)); and points from the model of Hudson and Mahle (300°K (open squares) 200K° (solid squares)).

cross-section. Measurements at many absorption minima were discarded because of this difficulty.

Results of measurements made at temperatures 300°K and 600°K by Hudson et al. [1966] are shown in Figure 3. No allowance was made in their measurements for the overlapping wings of absorption lines. Also shown are some points from the model of Hudson and Mahle [1972]. There are significant discrepancies in cases where the mode' of Hudson and Mahle is not directly related to measurements.

Calculations of the solar spectrum transmitted to any altitude in the atmosphere are complex in the region of the Schumann-Runge bands and are usually made by computing the absorption due to every spectral line in the system [e.g., Blake, 1979; Kockarts, 1976; Frederick and Hudson, 1980]. Continuum absorption in the region must also be accounted for, and the curves of Figure 3 provide adequate data for the detailed calculation of absorption in the Schumann-Runge continuum in that wavelength region for any model atmosphere. An algorithm that reproduces the cross-section at any temperature can be obtained from the authors.

The Schumann-Runge continuum is of particular significance for atmospheric photochemistry because it results in dissociation with one atom in the ^1D state. In the region discussed in this paper the continuum component of the total cross-section also corresponds to $O(^1D)$ formation, and the continuum strength could be measured directly in an experiment of the type conducted by Lee et al. [1977].

Acknowledgments. This work was supported by grants from the Australian Research Grants Committee and the U.S. Air Force Geophysics Laboratory. The authors wish to thank Mr. F. A. Smith for assistance in obtaining the experimental data.

The Editor thanks M. Ackerman and another referee for their assistance in evaluating this paper.

REFERENCES

Blake, A. J., An atmospheric absorption model for the Schumann-Runge bands of oxygen, J. Geophys. Res., 84, 3272, 1979.

Frederick, J. E., and R. D. Hudson, Dissociation of molecular oxygen in the Schumann-Runge bands, J. Atmos. Sci., 37, 1099, 1980.

Gies, H. P. F., S. T. Gibson, D. G. McCoy, A. J. Blake and B. R. Lewis, Experimentally determined oscillator strengths and linewidths for the Schumann Runge band system of molecular oxygen, III. The (7-0) to (19-0) bands, J. Quant. Spectrosc. Radiat. Transfer, 26, 469, 1981.

Herzberg, G., Spectra of Diatomic Molecules, Van Nostrand, New York, 1950.

Hudson, R. D., V. L. Carter, and J. A. Stein, An investigation of the effect of temperature on the Schumann-Runge absorption continuum of oxygen, 1580 - 1950Å, J. Geophys. Res., 71, 2295, 1966.

Hudson, R. D., and S. H. Mahle, Photodiscussion rates of molecular oxygen in the mesosphere and lower thermosphere, J. Geophys. Res., 77, 2902, 1972.

Jarmain, W. R., and R. W. Nicholls, A theoretical study of the O_2 $X^3\Sigma_g^-$ - $B^3\Sigma_u^-$ photodissociation continuum, Proc. Phys. Soc., 84, 417, 1964.

Kockarts, G., Absorption and photodissociation in the Schumann-Runge bands of molecular oxygen in the terrestrial atmosphere, Planet Space Sci., 24, 589, 1976.

Lee, L. C., T. G. Slanger, G. Black, and R. L. Sharpless, J. Chem. Phys., 67, 5602, 1977.

(Received April 1, 1982;
accepted May 10, 1982.)

J. Quant. Spectrosc. Radiat. Transfer Vol 26, No. 6, pp 469-481, 1981. Printed in Great Britain

Pergamon Press Ltd

EXPERIMENTALLY DETERMINED OSCILLATOR STRENGTHS AND LINEWIDTHS FOR THE SCHUMANN-RUNGE BAND SYSTEM OF MOLECULAR OXYGEN—III. THE (7–0) TO (19–0) BANDS

H. P. F. GIES, S. T. GIBSON, D. G. MCCOY, and A. J. BLAKE
Department of Physics, University of Adelaide, Adelaide, South Australia 5001

and

B. R. LEWIS
Research School of Physical Sciences, The Australian National University, Canberra, Australia 2600

(*Received* 18 *May* 1981)

Abstract—Experimental oscillator strengths and predissociation linewidths have been derived from equivalent width measurements at room temperature for the (11–0) to (15–0) Schumann–Runge bands of molecular oxygen, and at low temperature for the (15–0) to (19–0) bands, using the Adelaide 6 m vacuum ultraviolet monochromator operated at a resolution of 0.006 nm. Photometric methods were used to measure the ultraviolet absorption for 40 groups of rotational lines, and the resulting data were interpreted using a curve of growth type of analysis to give oscillator strengths and pre-dissociation linewidtns. The variation of the oscillator strengths with N'' within each band was found to agree well with the theoretical predictions of Allison, while the mean band oscillator strengths derived from the results are in good agreement with previous measurements. The results demonstrate the need for accurate data about multiplet line splittings. A revised analysis of previous data for the (7–0) to (14–0) bands is also presented.

INTRODUCTION

The absorption of ultraviolet light in the Schumann-Runge band system of molecular oxygen ($B^3\Sigma_u^- - X^3\Sigma_g^-$) has been studied extensively. Oscillator strengths of the various bands have been measured optically and can also be inferred from electron impact studies. These results were discussed fully by Lewis *et al.* who presented new photoelectrically determined oscillator strengths for the (v'–0) bands with $v' = 6 - 14$[1] and $v' = 2$–5.[2] Their high resolution work includes the first experimental measurements of the variation of band oscillator strength with N''. Previous theoretical work by Allison[3] had predicted this rotational variation, which has significance in the atmospheric absorption problem, as noted by Fang *et al.*[4]

The broadening of rotational lines in the Schumann-Runge bands due to predissociation of the $B^3\Sigma_u^-$ state has been observed by several experimenters. Theoretical discussions of the broadening have been compared with the measured linewidths by Lewis *et al.*[2] A modification of the predissociation model of Julienne[5] fits the data extremely well. Frederick and Hudson[6] have reported values of the linewidth for individual rotational lines which vary significantly within a band. Lewis *et al.*[7] after careful statistical analysis of their data, conclude that any variation of linewidth within a band must be considerably smaller than that reported by Frederick and Hudson.

This paper, a continuation of the work reported by Lewis *et al.*, presents high resolution photoelectric oscillator strength and predissociation linewidth measurements for a selection of lines in the (15–0) to (18–0) Schumann–Runge bands of molecular oxygen, and new measurements in the bands (11–0) to (14–0).

EXPERIMENTAL METHOD

A schematic diagram of the experimental apparatus with a 1 cm absorption cell that can be cooled to low temperatures is given is Fig. 1. The experimental method has been described in detail elsewhere.[1] Background continuum radiation (175–200 nm) provided by a thyratron triggered hydrogen discharge was dispersed by the Adelaide 6 m monochromator and monitored by a gated photomultiplier detection system before entering and after leaving the windowed absorption cell. Typical experimental wavelength resolution was 0.006 nm. The pressure of

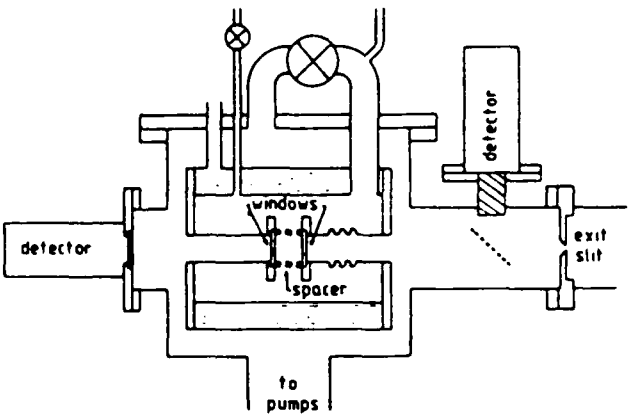

Fig. 1. A schematic diagram of the experimental arrangement, showing the double-walled absorption cell, which was cooled with a cryogenic liquid. The length of the absorption path is determined by a spacer, which separates the lithium fluoride windows.

oxygen in the absorption cell was servo-controlled and ranged from 1 to 300 torr for the lines studied in this work.

In normal operation, after the absorption line of interest had been located, wavelength scans were performed both with the cell evacuated, and with the cell filled to a suitable pressure with oxygen. Measurements were normally made at two widely differing pressures in order to allow the determination of both oscillator strength and linewidth.[1] However, some line groups, containing a mix of strong lines from neighbouring bands, were measured at several pressures, so that the contributions of these interfering lines could be more accurately evaluated.

The spectrum of the Schumann–Runge bands for $v' > 14$ is made complicated by perturbations and crowding of the lines. When making measurements of lines with $N'' < 13$, spectrum complexity was reduced by cooling the absorption cell ($T \sim 90$ K), thus reducing the strengths of many lines of higher rotational quantum number from higher bands allowing individual groups of lines to be accurately measured. To measure a variation of oscillator strength with rotational number, lines of higher N'' must be measured. High rotational number lines were selected at positions in neighbouring bands where the lines happened to fall clear of interference and the measurements were made at room temperature.

ANALYSIS OF DATA

The rotational absorption lines in the Schumann–Runge system exhibit a combination of both Doppler and Lorentz lineshapes, corresponding to thermal and predissociation broadening processes.[8] A mixing parameter a, which is the ratio of Lorentz to Doppler widths is used to characterise the line. From measurements of the line equivalent width at different pressures, both a and another dimensionless quantity $P'X$ (Penner[9])† can be found from a synthesised curve of growth.[1] The band oscillator strength $f(N'', v')$ obtained from measurement of a line with rotational number N'' and centre at wavelength λ_0(nm) is[1]:

$$f(N'', v') = 1.577 \times 10^{-7} T^{3/2} P' X / (P l \lambda_0 a S) \tag{1}$$

where T(K) is the temperature of the absorbing gas, P(torr) is the gas pressure, l(cm) is the absorbing path length, α is the weighted Boltzmann factor for the ground state rotational level giving rise to the line of interest, and S is the correctly normalised Hönl–London factor for the line. Theoretical calculation of $f(N'', v')$ involves evaluation of the integral:

$$\int \psi_{v'N'}(r) R_{v'}(r) \psi_{v''N''} \, dr \tag{2}$$

† P' is the true absorption coefficient at the centre of the equivalent Doppler line, and X is a measure of absorbing path

where $\psi_{v'N'}$ and $\psi_{v''N''}$ are the initial and final state vibrational wavefunctions, R_e is the electronic transition moment and r is the internuclear distance. If the integrand were independent of rotation, then the value obtained for the band oscillator strength would be the same for all lines in the band. However, the presence of the centrifugal term in the potential for a rotating molecule leads to rotationally dependent wavefunctions in Eq. (2). The $f(N'', v')$ will in general have a rotational dependence which will be seen when Eq. (1) is applied to experimental absorption data.

In this work, initial line centre wavelengths were taken from Brix and Herzberg[10] and Ackerman and Biaumé,[11] and weighted Boltzmann factors α were calculated from the $X^3\Sigma_g^-$ energy levels of Veseth and Lofthus.[12] Intermediate case (a–b) coupling Hönl–London factors were necessary for the lines nearer the band heads for the bands with $v' \geq 15$, otherwise case (b) Hönl–London factors were adequate. For the higher bands the separation of the P and R branches increases rapidly with N'', and this allowed isolated P or R branch triplets to be measured. In a few cases individual triplet components could be examined. At the same time, however, the higher bands increasingly tend to run together, and interference by strong lines from neighbouring bands is pronounced. All absorption processes which make any significant contribution over the wavelength range associated with an experimental scan must be taken into account in the construction of a curve of growth. Absorption may be due to neighbouring lines or to underlying continua. The single line analysis technique remains valid as long as the single line wavelength dependent absorption coefficient is replaced by the sum of the absorption coefficients for all the significant lines of interest in the scanned region.[1] Hence a knowledge of precise line positions and relative strengths is required for an accurate curve of growth to be constructed. Weak lines within the scan range were taken into account by explicitly adding these lines to the absorption model, and the contributions of strong lines outside the scan range were included by calculating an effective cross-section over the scan range. These strong lines contribute significantly to the absorption because of the Lorentz component of their wings, but uncertainty in the assumed parameters results in only second order errors in the synthesised equivalent width. In calculating the equivalent width the wavelengths of the lines making a major contribution were taken from Brix and Herzberg[10] and Ackerman and Biaumé.[11] Wavelengths of all other lines were calculated from the spectroscopic constants given by Bergeman and Wofsy,[13] and their linewidths were taken from Hudson and Mahle.[14]

In the region of the higher bands a temperature dependent Schumann–Runge continuum, corresponding to population of the rotational levels of the $X^3\Sigma_g^-$ state, underlies the absorption lines. Absorption coefficients were measured at numerous positions between rotational lines, where other contributions were small, and a model fitted to ther results.[15] This model was then used to give values of absorption coefficient for the continuum.

All the above factors were combined into a computer programme, which generated the values of the oscillator strength and predissociation linewidth for a reference line in the group of lines which was scanned, by a convergent iterative process using approximate initial values. The programme also produced a convolution of the instrumental profile and the theoretical absorption profile for comparison with the experimental output data. When the calculated and measured absorption profiles were in agreement for all pressures, the analysis was assumed to be reliable.

The higher bands contain perturbed lines, only a few of which have been tentatively identified by Brix and Herzberg.[10] Because these lines are of undefined strength, or because some weak lines may not have been measured, the synthesised equivalent width may be unreliable. Agreement between the synthesised and experimentally observed absorption profiles was used as an indication that the error introduced by unidentified lines was small.

In bands higher than (15–0) the line positions calculated using the molecular constants were often in error because of perturbations†, and agreement between the synthesised and experimental absorption profiles was in some cases improved by making adjustments to the wavelengths of major lines for which no measured wavelength was available.

In many cases the wavelengths of individual triplet components have not been observed, so that the splitting of these lines is unknown. The equivalent width for a pair of lines is insensitive

†Details of these shifted lines will be published.

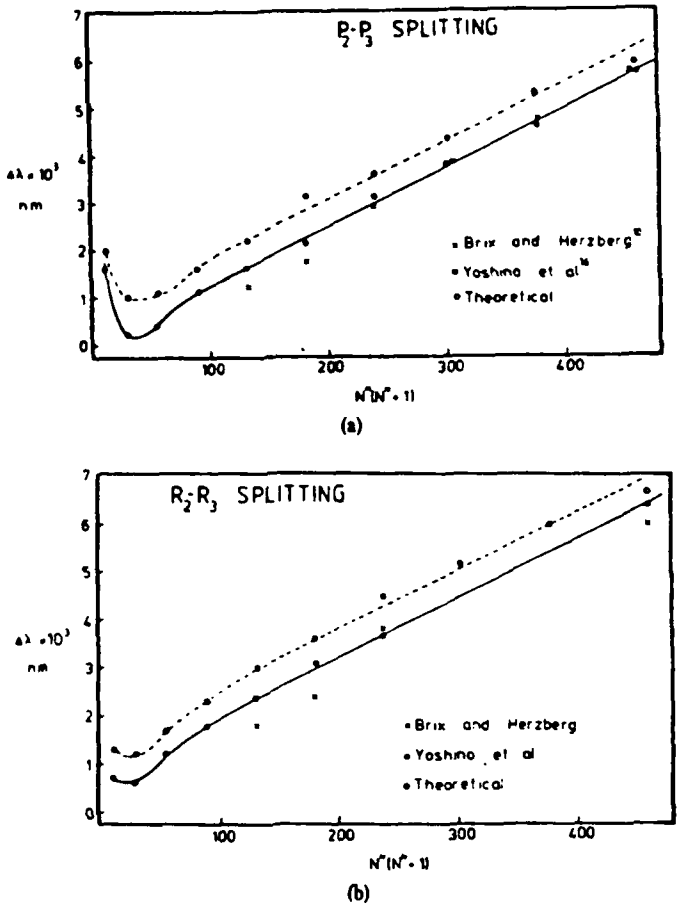

Fig. 2. A comparison of the observed triplet splittings of Brix and Herzberg[10] and Yoshino *et al.*[16] with the triplet splittings calculated from the molecular constants of Bergeman and Wofsy[13], as a function of rotational number N''. The linewidth for the (14–0) band rotational lines is approximately 0.7×10^{-3} nm (full width at half maximum).

to the line separation either when the separation is very small or very large compared with the linewidth, but for intermediate cases, the equivalent width is very sensitive to these parameters. This critical dependence on triplet splitting arises in the (13–0) and (14–0) bands. Brix and Herzberg[10] were unable to give triplet splittings for lines with $N'' \leq 9$ in these bands. Calculations using the spectroscopic constants of Bergeman and Wofsy[13] give splittings of order of 0.001–0.002 nm, compared with the linewidths of about 0.0007 nm. Since the reliability of these calculated splittings was unknown, previous results[1] were analysed on the assumption that the P_2–P_3 and R_2–R_3 splittings were zero. New, but preliminary, measurements of the (14–0) band by Yoshino *et al.*[16] resolved some of these lines and they report splittings significantly smaller than those calculated with the spectroscopic constants. Use of these data had the effect of decreasing the derived oscillator strengths for lines with low N'', while those for large N'' remained unchanged. The line splitting data for the (14–0) band is summarised in Fig. 2.

RESULTS

(i) *Oscillator strengths*

The measured values of P and R branch oscillator strengths are presented in Table 1. In all except a few cases P and R branch lines were measured independently. For those cases where unresolved $P(N'')$, $R(N''+2)$ groups were studied, the analysis was made using the ratio of the P and R branch oscillator strengths calculated by Allison.[3] There is good agreement between the calculated P/R oscillator strength ratio and the measured value when independent measurements could be made.

Table 1. Band oscillator strengths $f(N'', v')$ for the (7–0) to (19–0) bands: (a) P-branch, (b) R-branch. The bracketed values in Table 1(b) are calculated from measured P-branch oscillator strengths using the ratio of strengths R/P. Values for the bands (7–0) to (10–0) were obtained by correcting previous data. Isolated line measurements for the (20–0) and (21–0) are also included. Values marked * are also adopted as mean band oscillator strengths.

(a)

N'' \ v'	7	8	9	10	11	12	13
3	0.342 ± 0.017	0.707 ± 0.037	1.06 ± 0.06	1.40 ± 0.10			
5	0.385 ± 0.020	0.714 ± 0.039	1.17 ± 0.09	1.42 ± 0.10	2.20 ± 0.09	2.80 ± 0.10	2.91 ± 0.18
7	0.405 ± 0.025	0.681 ± 0.037	1.25 ± 0.11	1.53 ± 0.09	2.31 ± 0.09	2.97 ± 0.12	2.81 ± 0.14
9	0.389 ± 0.019	0.735 ± 0.036	1.19 ± 0.07	1.38 ± 0.08	2.27 ± 0.09	2.84 ± 0.12	2.82 ± 0.14
11	0.388 ± 0.021	0.677 ± 0.044	1.08 ± 0.07	1.68 ± 0.09	2.36 ± 0.09	2.74 ± 0.12	2.89 ± 0.10
13	0.339 ± 0.022	0.683 ± 0.041	1.10 ± 0.07	1.64 ± 0.13	2.43 ± 0.10	2.70 ± 0.12	2.96 ± 0.40
15	0.335 ± 0.023	0.690 ± 0.042	1.13 ± 0.09	1.55 ± 0.11	1.94 ± 0.08	2.61 ± 0.10	2.86 ± 0.10
17	0.353 ± 0.023	0.650 ± 0.035	1.06 ± 0.08	1.55 ± 0.10	2.18 ± 0.08	2.61 ± 0.11	
19	0.364 ± 0.017	0.660 ± 0.028	1.07 ± 0.05	1.65 ± 0.10	2.10 ± 0.09		
21	0.300 ± 0.016	0.613 ± 0.031	0.99 ± 0.05	1.43 ± 0.08			
23	0.302 ± 0.019	0.558 ± 0.028			1.69 ± 0.11		
25	0.291 ± 0.013				1.63 ± 0.09	2.00 ± 0.09	2.30 ± 0.25
27							
29							
31				0.73 ± 0.04			

N'' \ v'	14	15	16	17	18	19
3			2.94 ± 0.15	2.78 ± 0.16	2.75 ± 0.10	
5	3.48 ± 0.40	2.87 ± 0.13	2.86 ± 0.13	2.94 ± 0.10	1.99 ± 0.10	1.43 ± 0.35
7	3.25 ± 0.15	3.24 ± 0.19	2.63 ± 0.11	2.71 ± 0.17	2.21 ± 0.10	1.60 ± 0.09
9	3.30 ± 0.23	3.10 ± 0.12	2.92 ± 0.20	2.74 ± 0.22		
11	3.31 ± 0.20	2.67 ± 0.09	2.78 ± 0.14			
13	3.32 ± 0.30	3.13 ± 0.22		2.33 ± 0.15		
15	3.02 ± 0.17		2.28 ± 0.09	2.62 ± 0.20		
17			1.73 ± 0.08			
19	2.40 ± 0.13	2.57 ± 0.14				
21	2.43 ± 0.40		2.19 ± 0.09			
23			2.26 ± 0.20			
25						
27	2.33 ± 0.19					
29						
31						

Table 1 (*Contd*)

(b)

$M^{V'}$	7	8	9	10	11	12	13
1							
3							
5	(0.337 ± 0.017)	(0.696 ± 0.037)	(1.05 ± 0.06)	(1.38 ± 0.10)			
7	(0.376 ± 0.020)	(0.697 ± 0.099)	(1.14 ± 0.08)	(1.39 ± 0.10)		2.85 ± 0.12	2.81 ± 0.14
9	(0.393 ± 0.025)	(0.660 ± 0.037)	(1.21 ± 0.10)	1.49 ± 0.09	1.93 ± 0.08	2.70 ± 0.09	2.73 ± 0.16
11	(0.374 ± 0.019)	(0.707 ± 0.036)	(1.14 ± 0.07)	1.62 ± 0.11	2.06 ± 0.08	2.54 ± 0.10	2.70 ± 0.10
13	(0.371 ± 0.021)	(0.647 ± 0.044)	1.04 ± 0.08	1.58 ± 0.12	2.20 ± 0.10	2.51 ± 0.10	3.00 ± 0.40
15	(0.321 ± 0.022)	(0.647 ± 0.041)	1.01 ± 0.06	1.29 ± 0.10	2.08 ± 0.08	2.78 ± 0.12	3.00 ± 0.35
17	(0.315 ± 0.023)	(0.649 ± 0.042)	1.23 ± 0.08	1.25 ± 0.10	1.84 ± 0.07	2.53 ± 0.11	2.86 ± 0.20
19	(0.330 ± 0.023)	(0.607 ± 0.035)	0.91 ± 0.06	1.43 ± 0.08	1.94 ± 0.08	2.67 ± 0.11	
21	(0.337 ± 0.017)	0.560 ± 0.036	1.02 ± 0.06	1.31 ± 0.07	1.82 ± 0.08		
23	(0.276 ± 0.016)	0.620 ± 0.043	0.99 ± 0.07				
25	(0.275 ± 0.019)	0.517 ± 0.34		0.78 ± 0.04		2.02 ± 0.07	2.14 ± 0.14
27	(0.263 ± 0.013)						
29				0.79 ± 0.04			

$M^{V'}$	14	15	16	17	18	19	20	21
1								1.38 ± 0.40
3					2.23 ± 0.25		1.52 ± 0.30	0.93 ± 0.20*
5		3.31 ± 0.23	2.98 ± 0.12	2.78 ± 0.11	2.03 ± 0.25	1.32 ± 0.20		
7	3.18 ± 0.15	2.89 ± 0.16	2.98 ± 0.19	2.39 ± 0.09	1.63 ± 0.10	1.53 ± 0.08		
9	3.74 ± 0.20	3.00 ± 0.12	2.79 ± 0.12	2.91 ± 0.20			0.73 ± 0.03*	
11	3.29 ± 0.13	3.14 ± 0.12	2.62 ± 0.13					
13	.69 ± 0.30	3.35 ± 0.20						
15	3.20 ± 0.22		2.33 ± 0.11	2.94 ± 0.16				
17		2.19 ± 0.06						
19		2.10 ± 0.08						
21	2.71 ± 0.25	2.25 ± 0.16						
23								
25								
27	2.34 ± 0.22							
29								

New measurements of oscillator strengths for the (11–0) to (14–0) bands made in the present work showed discrepancies with values previously reported[1] which were made with a different apparatus. The discrepancies which remained after differences in the assumptions about line splittings had been taken into account were found to be due to an unexpected pressure gradient in the apparatus previously used, which particularly affected the measurement of low pressures. Careful recalibration allowed a reanalysis of the previous data, and the oscillator strengths and linewidths obtained are in good agreement with those obtained from the new measurements.

Figures 3 and 4 show a comparison of the experimentally measured oscillator strengths for the (11–0) and (15–0) bands with those predicted by Allison.[3] Except for lines near the band origin, the band oscillator strengths calculated by Allison can be represented by an expression of the form:

$$f(N'', v') = f_0(v') - \beta(v')N''(N''+1) \tag{3}$$

where f_0 is the band oscillator strength for no rotation and β gives the rotational dependence. Evaluation of the integral in Eq. (2) using wavefunctions obtained from the potential for a rotating molecule made during the present work support the form of this rotational dependence.

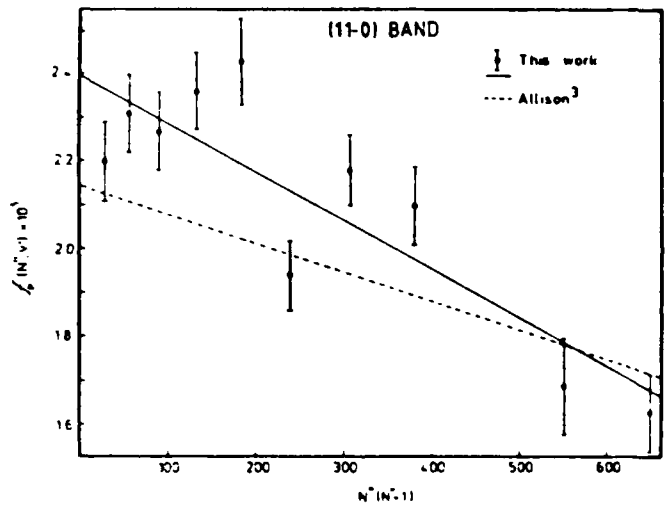

Fig. 3. The band oscillator strength $f(N'', v')$ vs $N''(N''+1)$ for the (11–0) band P-branch. The dashed line is the theoretical prediction of Allison[3].

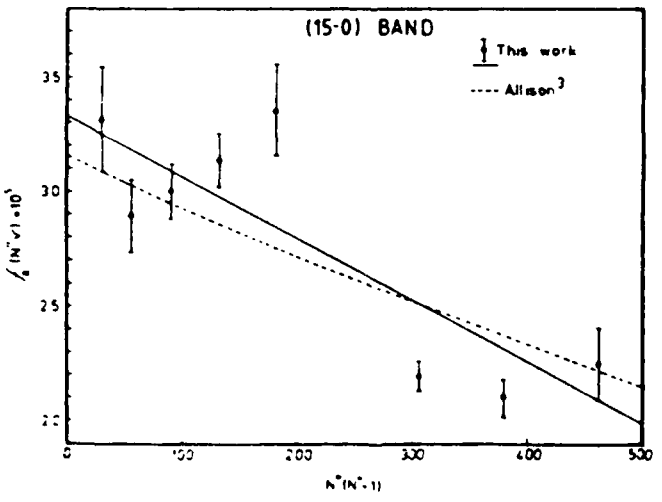

Fig. 4. The band oscillator strength $f(N'', v')$ vs $N''(N''+1)$ for the (15–0) band R-branch, compared with the predictions of Allison[3] (dashed line).

Values of f_0 and β for the bands (5–0) to (17–0) have been calculated by least squares fitting of Eq. (3) to the experimental results of Table 1. These values, together with those obtained from the calculations of Allison, are presented in Table 2. The results are in good agreement, and confirm the general tendency for β to increase with increasing v'. This can be seen in Fig. 5, where $\beta/f_0(v')$ is plotted as a function of v'. It would appear from these results that the centrifugal term in the potential, the parameters of which are fixed by the molecular constants, adequately accounts for the rotational dependence of the band oscillator strength.

The present band oscillator strengths obtained from individual lines can be compared with band strengths obtained by previous workers who used a low resolution technique to measure band absorption provided that explicit account is taken of the temperature dependence of those measurements. Their results represent a weighted mean of the band oscillator strengths obtained from individual rotational lines. By weighting each $f(N'', v')$ with the appropriate Boltzmann factor this mean band oscillator strength can be calculated for any temperature. Table 3 and Fig. 6 present mean band oscillator strengths obtained from the data in Table 1 for a temperature of 300 K for comparison with the results of Ditchburn and Heddle,[17] Bethke,[18] Hudson and Mahle,[14] Heubner [19] and Frederick and Hudson[6] which extend as far as the (17–0) band, and with the theoretical predictions of Allison.[3]

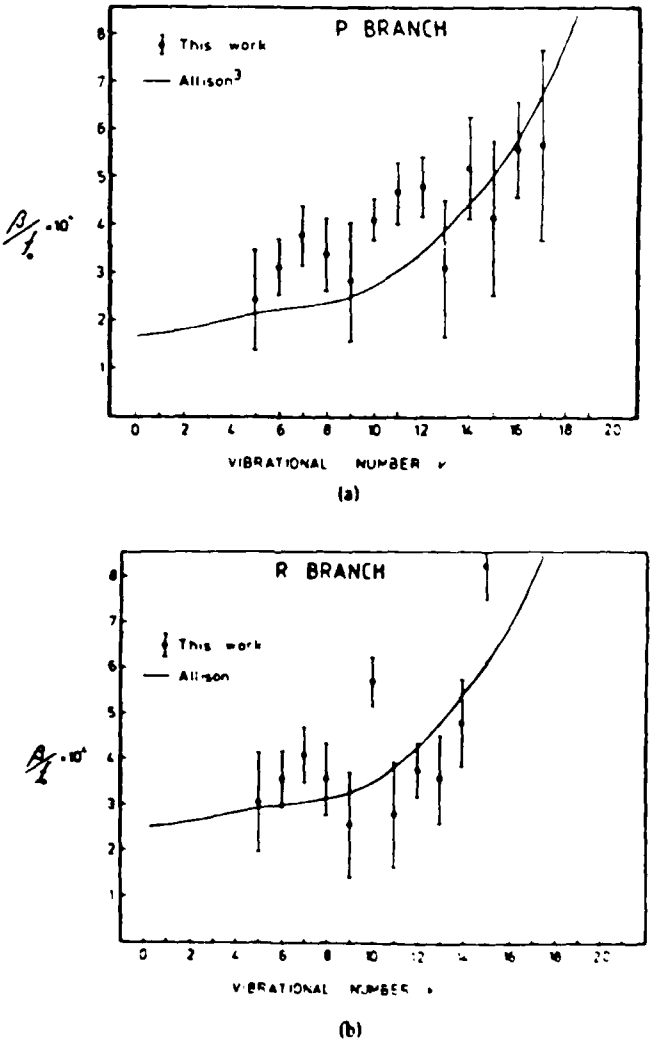

Fig. 5. The rate of change of oscillator strength with rotation ($\beta'/f_0(v')$) as a function of the vibrational number v'. The line represents the theoretical predictions of Allison[3] (a) P branch (b) R branch

Table 2. Values of f_0 and β of Eq. 3 from the present measurements and the theoretical work of Allison[3].

	$f_e(v) \times 10^3$				$\beta \times 10^6$			
	P Branch		R Branch		P Branch		R Branch	
BAND	THIS WORK	ALLISON	THIS WORK	ALLISON	THIS WORK	ALLISON	THIS WORK	ALLISON
7-0	0.387 ± 0.009	0.377	0.381 ± 0.01	0.372	0.145 ± 0.03	0.0862	0.156 ± 0.22	0.114
8-0	0.724 ± 0.018	0.674	0.708 ± 0.02	0.665	0.248 ± 0.06	0.159	0.252 ± 0.57	0.207
9-0	1.17 ± 0.04	1.08	1.14 ± 0.04	1.07	0.329 ± 0.15	0.270	0.292 ± 0.13	0.349
10-0	1.63 ± 0.04	1.59	1.58 ± 0.05	1.57	0.667 ± 0.07	0.436	0.899 ± 0.09	0.551
11-0	2.41 ± 0.05	2.15	2.13 ± 0.07	2.11	1.13 ± 0.15	0.662	0.591 ± 0.25	0.821
12-0	2.96 ± 0.06	2.68	2.85 ± 0.06	2.64	1.42 ± 0.18	0.937	1.06 ± 0.17	1.14
13-0	2.99 ± 0.10	3.08	3.00 ± 0.10	3.03	0.923 ± 0.44	1.23	1.07 ± 0.29	1.47
14-0	3.44 ± 0.13	3.27	3.64 ± 0.14	3.21	1.78 ± 0.37	1.49	1.74 ± 0.35	1.76
15-0	3.12 ± 0.10	3.19	3.34 ± 0.06	3.12	1.28 ± 0.51	1.65	2.73 ± 0.26	1.93
16-0	2.84 ± 0.08	2.94	3.10 ± 0.11	2.88	1.58 ± 0.29	1.68	3.29 ± 0.75	1.96
17-0	2.85 ± 0.10	2.57		2.50	1.61 ± 0.86	1.75		2.00
18-0		2.10		2.04		1.67		1.92
19-0		1.61		1.56		1.71		1.97
20-0		1.07		1.02		1.58		1.79
21-0		0.695		1.078		1.53		2.33

Table 3. Mean band oscillator strengths f obtained from the present measurements compared with some previous measurements, and the theoretical values of Allison[3].

BAND	BETHKE[1,6]	HUDSON & MAHLE[1,6]	HUEBNER[1,6] et al	FREDERICK[4] & HUDSON	ALLISON[3]	THIS WORK
7-0	0.356	0.35	0.35	0.315	0.361	0.368 ± 0.01
8-0	0.675	0.60	0.685	0.578	0.645	0.692 ± 0.02
9-0	1.07	1.0	1.05	1.04	1.03	1.13 ± 0.05
10-0	1.56	1.6	1.60	2.60	1.51	1.52 ± 0.04
11-0	2.16	1.7	2.26	1.80	2.03	2.16 ± 0.05
12-0	2.81	2.5	2.88	2.09	2.52	2.74 ± 0.06
13-0	3.17	4.5	3.41	2.69	2.88	2.87 ± 0.12
14-0	3.24	5.0	3.77		3.01	3.21 ± 0.14
15-0	3.26	3.1	3.73		2.91	2.95 ± 0.12
16-0	3.16	2.5	3.53		2.67	2.63 ± 0.08
17-0	2.95		3.03		2.29	2.64 ± 0.15
18-0			2.72		1.84	2.14 ± 0.15
19-0			1.98		1.34	1.47 ± 0.13
20-0			1.64		0.82	0.73 ± 0.08
21-0					0.43	0.93 ± 0.20

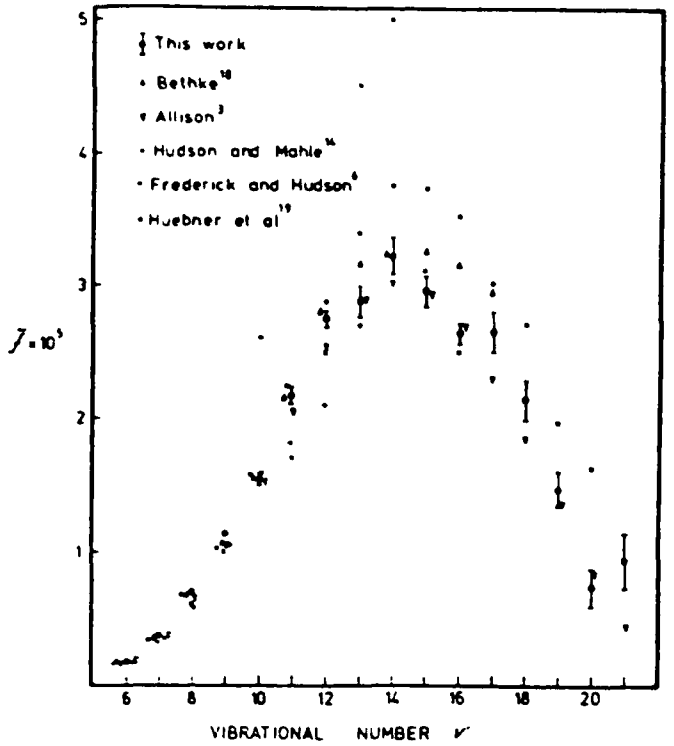

Fig. 6. A comparison of the mean band oscillator strengths $\bar{f}$ of this work with those of previous experimenters, and the theoretical values of Allison[3].

(ii) *Predissociation linewidths*

Predissociation linewidths were obtained for all lines for which oscillator strengths are given in Table 1. The predissociation linewidths for individual rotational lines for the (8–0) to (18–0) bands, were measured. There is no statistically significant variation of line width within any of the bands, in agreement with the conclusions of Lewis *et al.*[7] Average linewidths for each band are presented in Table 4 and Fig. 7 for comparison with previously published results.[6,11,14] Theoretically calculated linewidths from the work of Julienne and Krauss[21] and Julienne[5] show

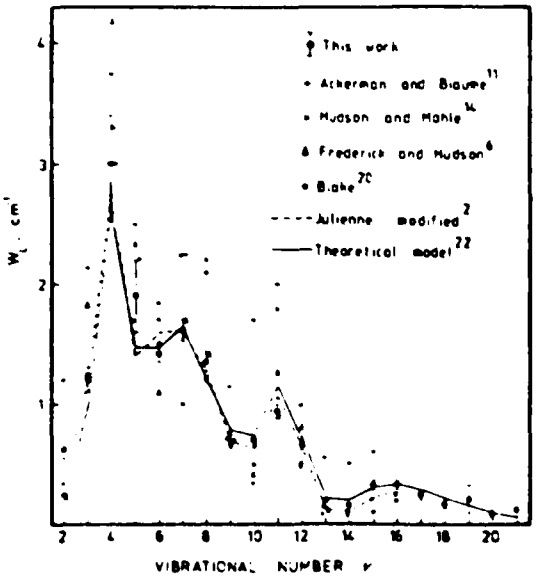

Fig. 7. A comparison of the mean predissociation linewidth $\bar{W}_J$ (full width at half maximum) for each band obtained in this work with the results of previous experimenters.

Table 4. Mean predissociation linewidths W_L (full width at half maximum) in cm^{-1} for each band.

BAND	ACKERMAN & RIAUME[11]	HUDSON & MAILE[14]	BLAKE[10]	FREDERICK & HUDSON[9]	JULIENNE (Modified)[3]	THEORETICAL MODEL[13]	THIS WORK
7-0	2.25	2.25	1.0	1.70	1.60	1.64	1.62 ± 0.10
8-0	2.1	2.21	1.2	1.43	1.27	1.21	1.36 ± 0.09
9-0	1.15	0.72	0.7	0.56	0.69	0.79	0.67 ± 0.04
10-0	1.7	0.54	0.5	0.42	0.61	0.74	0.70 ± 0.04
11-0	2.0	1.80	0.9	1.27	1.06	1.14	0.94 ± 0.06
12-0	1.0	0.48	0.5	0.812	0.63	0.69	0.66 ± 0.03
13-0	0.55	0.08	0.15	0.132	0.12	0.22	0.20 ± 0.005
14-0	0.5	0.06	0.1		0.10	0.20	0.16 ± 0.02
15-0	0.6	0.20	0.1		0.22	0.30	0.32 ± 0.04
16-0		0.25	0.2		0.29	0.32	0.33 ± 0.03
17-0						0.28	0.25 ± 0.03
18-0						0.22	0.16 ± 0.03
19-0						0.15	0.22 ± 0.12
20-0						0.10	0.08 ± 0.04
21-0						0.06	0.125± 0.06

significant departures from the present results. Values obtained by adjusting the parameters[3] of the model used by Julienne shown in Fig. 7 are in good agreement. Also shown in Fig. 7 are linewidths obtained from calculations[22] of Franck–Condon factors for predissociation made using an independent model for the potential curves. The measured widths were fitted by treating the electronic matrix element, the positions of the repulsive potential curves and their slopes as parameters. No previous measurements have been reported for the linewidths of bands higher than (16–0).

CONCLUSIONS

The present work completes a detailed study of the Schumann–Runge bands between (2–0) and (19–0). Comparisons of the variation of the band oscillator strength with rotational number, and of the linewidth with vibrational number, with recent theoretical work, indicate that the absorption processes are well understood, and that these results can be used to accurately model the atmospheric absorption of solar radiation.

Further study of the bands with $v' < 2$ and $v' > 18$ is needed, and each region presents particular difficulties. The lower bands are very weak and the lines are predominantly Doppler broadened so that the presence of predissociation cannot be inferred from observations of the lineshape. The higher bands feature crowding of the lines and strong perturbations which make interpretation of the absorption data difficult.

Acknowledgements—This work was supported by grants from the Australian Research Grants Committee and the U.S Airforce Office of Scientific Research. The authors would also like to thank F. A. Smith for his valuable assistance during the course of this work.

REFERENCES

1. B. R. Lewis, J. H. Carver, T. I. Hobbs, D. G. McCoy, and H. P. F. Gies, *JQSRT* **20**, 191 (1978).
2. B. R. Lewis, J. H. Carver, T. I. Hobbs, D. G. McCoy, and H. P. F. Gies, *JQSRT* **22**, 213 (1979).
3. A. C. Allison, Private communication (1975).
4. T. M. Fang, S. C. Wofsy, and A. Dalgarno, *Planet. Space Sci.* **22**, 413 (1974).
5. P. S. Julienne, *J. Molec. Spectrosc.* **63**, 60 (1976).
6. J. E. Frederick and R. D. Hudson, *J. Molec. Spectrosc.* **74**, 247 (1979).
7. B. R. Lewis, J. H. Carver, T. I. Hobbs, D. G. McCoy, and H. P. F. Gies, *JQSRT* **24**, 365 (1980).
8. R. D. Hudson and V. L. Carter, *J. Opt. Soc. Am.* **58**, 1621 (1968).
9. S. S. Penner, *Quantitative Molecular Spectroscopy and Gas Emissivities* Addison-Wesley, Reading (1959).
10. P. Brix and G. Herzberg, *Can. J. Phys.* **32**, 110 (1954).
11. M. Ackerman and F. Biaumé, *J. Molec. Spectrosc.* **35**, 73 (1970).
12. L. Veseth and A. Lofthus, *Molec. Phys.* **27**, 511 (1974).
13. T. H. Bergeman and S. C. Wofsy, *Chem. Phys. Lett.* **15**, 104 (1972).
14. R. D. Hudson and S. H. Mahle, *J. Geophys. Res.* **77**, 2902 (1972).
15. H. P. F. Gies, S. T. Gibson, A. J. Blake, and D. B. McCoy. To be published in *JQRST*.
16. K. Yoshino, D. E. Freeman, and W. H. Parkinson. Private Communication (1980).
17. R. W. Ditchburn and D. W. O. Heddle, *Proc. R. Soc.* **226A**, 509 (1954).
18. G. W. Bethke, *J. Chem. Phys.* **31**, 669 (1959).
19. R. H. Huebner, R. J. Celotta, S. R. Mielczarek, and C. E. Kuyatt, *J. Chem. Phys.* **63**, 241 (1975).
20. A. J. Blake, *J. Geophys. Res.* **84**, 3222 (1979).
21. P. S. Julienne and M. Krauss, *J. Molec. Spectrosc.* **56**, 270 (1975).
22. S. T. Gibson, A. J. Blake, and D. G. McCoy. To be published in *JQSRT*.

JOURNAL OF GEOPHYSICAL RESEARCH, VOL. 88, NO. A1, PAGES 500-502, JANUARY 1, 1983

TRANSMITTANCE OF THE ATMOSPHERE IN THE (8-0) AND (9-0) SCHUMANN-RUNGE BANDS OF OXYGEN

S. T. Gibson, H. P. F. Gies,[1] A. J. Blake, and D. G. McCoy

Department of Physics, University of Adelaide,
Adelaide, South Australia 5000, Australia

Abstract. Dissociation rate constants for absorption by atmospheric oxygen in the Schumann-Runge bands are usually calculated by making line by line calculations of the absorption cross section. The accuracy of the cross sections used in these calculations needs to be tested against experimental data. A transmittance spectrum computed by using a detailed model cross section is compared with a spectrum recorded in the atmosphere and another recorded in the laboratory. It is concluded that details of the atmospheric absorption spectrum can be reproduced with excellent accuracy by the computed cross section.

Introduction

Absorption of solar ultraviolet radiation by oxygen in the region of the predissociated Schumann-Runge bands is an important source of atomic oxygen in the stratosphere and lower thermosphere [Hudson and Carter, 1969], but precise calculations of the solar spectrum transmitted to any altitude are made difficult by the complexity of the band system. Dissociation rate constants for this spectral region are obtained by calculating the transmittance spectrum with a detailed model of the cross section that takes account of the profile of every absorption line and all continuum absorption processes [Ackerman et al., 1970; Fang et al., 1974; Kockarts, 1976; Blake, 1979; Frederick and Hudson, 1980]. Temperature effects in the cross section are important and they can be included explicitly in the calculations [Ackerman et al., 1970; Kockarts, 1971, 1976; and Blake, 1979].

The cross sections that have been developed for this purpose are based on data for fundamental molecular parameters. Wavelengths for the absorption lines can be calculated from the values for the vibrational energies, the rotational constants and the multiplet splitting constants. Experimentally determined line positions can be used in many cases. Line profiles are calculated by using data for the band oscillator strengths with the appropriate Honl-London factors and data for the predissociation line widths. Various semiempirical models have been used by different authors for the underlying Schumann-Runge and Herzberg continua.

The accuracy of the model cross sections is limited by the errors in the laboratory data that are used. There are, for example, significant discrepancies between the various measurements of the band oscillator strengths, and not all models have included the rotational dependence of these quantities [Gies et al., 1981]. Another uncertainty in the higher bands arises from the presence of perturbations and unidentified lines in the band system [Gies et al., 1981].

Tests of the accuracy of the cross section can be made by performing a convolution of the computed transmittance spectrum with the instrumental profile to synthesise the result of any experimental measurement [Blake, 1979]. Solar spectra transmitted by the atmosphere to various altitudes have been recorded from rockets and balloons [Longmire et al., 1979; Frederick et al.,1981; Hall, 1981]. These spectra provide an excellent test of the cross sections used in aeronomic calculations.

Frederick et al. [1981] reported such a comparison with their measurements of atmospheric transmittance in the region of the lower Schumann-Runge bands that were made from a balloon at altitudes up to 39 km with a resolution of 0.3 nm. The purpose of this paper is to demonstrate the detailed accuracy of a model cross section by comparison of the calculated atmospheric transmittance with a measurement of the spectrum at 85 km by Longmire et al. [1979] using a rocket-borne spectrograph with a wavelength resolution (FWHM) of 0.012 nm. The value of such a comparison has been pointed out by Kockarts [1981].

Calculations of the Transmittance

The model for the absorption cross section in the Schumann-Runge bands used to calculate the transmittance spectrum was similar to the one reported by Blake [1979]. The line positions were calculated by using data for molecular constants and in the spectral region concerned here the calculated positions agree with those obtained from spectroscopic measurements to an accuracy better than 0.001 nm. Line strengths were obtained from the rotationally dependent band oscillator strength data of Gies et al. [1981] and intermediate coupling Honl-London factors. Each line was assumed to have a Voigt profile and the predissociation linewidths of Gies et al. [1981] were used in computing the profile. The cross section was computed at intervals of 0.002 nm. At each wavelength the contributions from all absorption lines with centers within 200 cm^{-1} of that wavelength were summed. Absorption in the Herzberg continuum was calculated with the model used by Blake [1979] and the model for the Schumann-Runge continuum for the region of the higher bands developed by Gies et al. [1982] was used.

Calculations of the transmittance spectrum at 85 km were made by approximating the atmosphere above 85 km to a single isothermal layer and

[1] Now at The Australian Radiation Laboratory, Yallambie, Victoria 3085, Australia.

Paper number 2A1609.
0148-0227/83/002A-1609$02.00

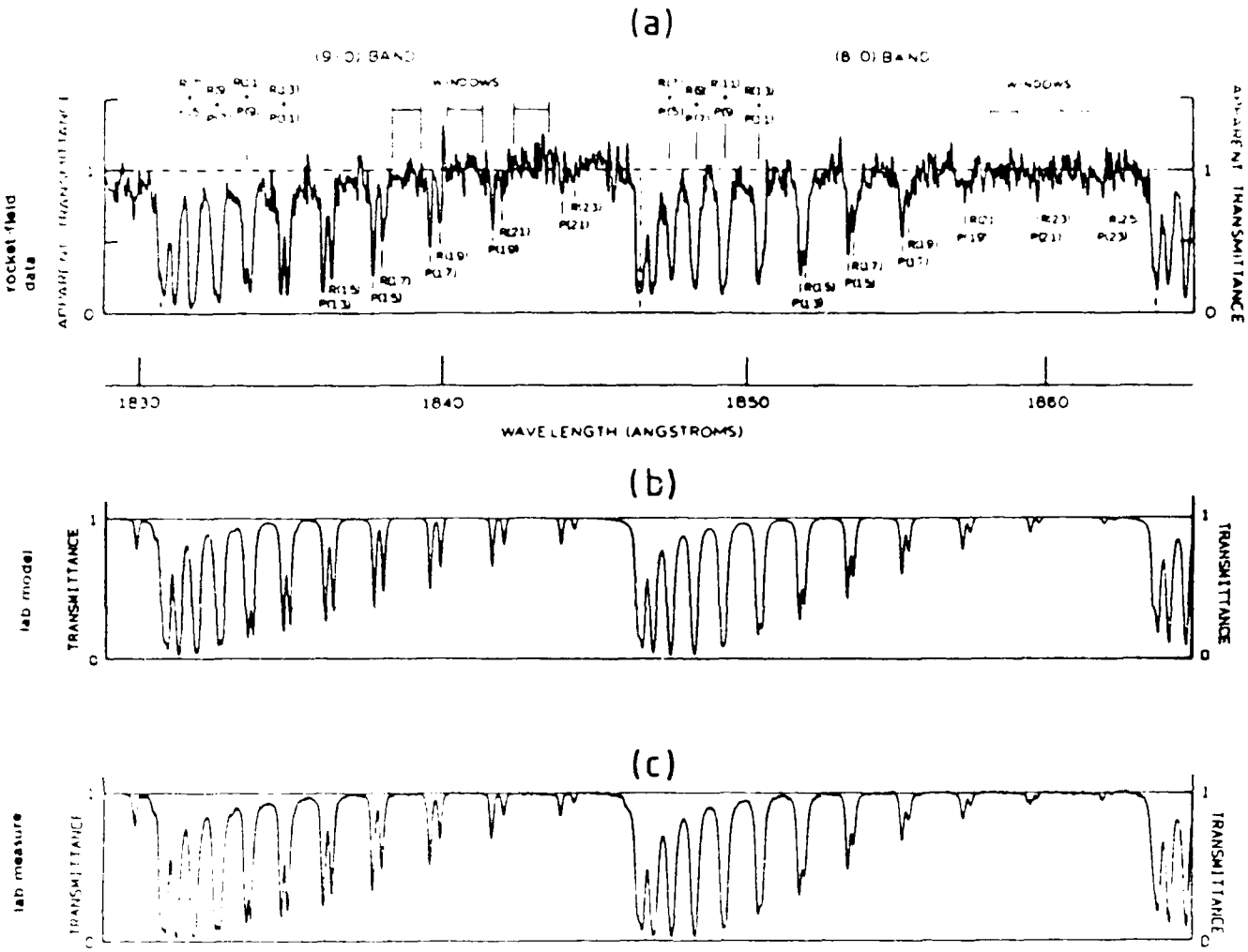

Fig. 1. (a) Apparent transmittance of the atmosphere at 85 km along a line with zenith angle 53.6°, reproduced from Figure 1 of Longmire et al. [1979]; (b) and (c) are transmittance spectra in the (8-0) and (9-0) Schumann-Runge bands of oxygen calculated from a model absorption cross section and measured in the laboratory, respectively. Both (b) and (c) correspond to an instrumental bandwidth of 0.012 nm and an oxygen column density of 2.0×10^{19} cm^{-2} at a temperature of 190°K.

computing the cross section for the appropriate temperature. A single layer is adequate at this altitude because the atmospheric temperature does not change significantly for more than a scale height above 85 km. The calculations were made for a solar zenith angle of 54°, corresponding to the conditions under which the spectrum of Longmire et al.[1979] was recorded.

Computed transmittance spectra for several different values of temperature and vertical column density were convoluted with a Gaussian profile with a width at half height of 0.012 nm to obtain spectra that could be compared directly with the atmospheric spectrum. The spectrum reported by Longmire et al. and a computed spectrum in the region of the (8-0) and (9-0) bands are shown in Figures 1a and 1b respectively.

Laboratory Measurements

Also shown, in Figure 1c, is a transmittance spectrum measured in the laboratory under conditions which simulate those in the atmosphere above 85 km. The measurements were made by using a 6.7-m vacuum monochromator with slit widths adjusted to give a wavelength resolution of 0.012 nm the same as that of the spectrograph used by Longmire et al. An absorption cell with a length of 1 cm was cooled by using a cryogenic liquid [Gies et al., 1981] and the transmittance spectrum was recorded for several different values of the sample gas pressure and temperature.

Discussion

The resolution of the spectrum of Longmire et al. is high enough to partly resolve the rotational structure of the (8-0) and (9-0) bands, and it thus provides a test of the ability of the model cross section to reproduce this structure. It is particularly important that such a test should be made because the distribution of absorption rate with altitude depends strongly on the fine structure of the cross section, rather

than the average cross section for any region. The minimum cross section between two rotational lines is sensitive to the relative positions of the lines and the widths of their profiles.

The calculated and laboratory transmittance spectra shown in Figures 1b and 1c respectively, correspond to a temperature of 190°K and a vertical column density of $2.0 \times 10^{19} cm^{-2}$ These values are the effective temperature assumed by Longmire et al. for the atmosphere above 85 km and the average column density they derived from analysis of spectra in several bands with several absorption models. It was found that the details of each laboratory spectrum were reproduced with excellent accuracy by the calculated spectrum corresponding to the same temperature and column density.

Comparison of the spectra in Figures 1a and 1b shows excellent overall agreement, but there are several detailed discrepancies. The strengths of the P(5)R(7) and P(7)R(9) absorption lines of the (8-0) band in Figure 1a are anomalous and examination of Figure 1 in Longmire et al. [1979] indicates that this may result from errors in the analysis of the original spectra caused by the coincidence of Fraunhofer lines with these absorption lines. Other discrepancies in line strengths are no greater than expected from random noise in Figure 1a. Comparison of the spectra also indicates that the true 100% transmittance line in Figure 1a should be lower than shown near the (9-0) band head, and higher near the (8-0) band head.

It was not possible to determine either the atmospheric temperature or the column density with any useful degree of accuracy from a visual comparison of the atmospheric transmittance spectrum with computed spectra because of the noise in the atmospheric spectrum. Longmire et al. determined the column density by comparing the integrated absorption over a band with that obtained from a model calculation at an assumed temperature. It appears that the accuracy of that process might be improved by careful comparison of the atmospheric spectra with a detailed computed spectrum so that effects of obvious faults in the data can be eliminated.

The calculation of dissociation rates for atmospheric oxygen by solar radiation in the region of the Schumann-Runge bands involves uncertainties in data for the absorption cross section, the atmospheric structure and the solar spectrum. The accuracy of the first calculations of dissociation rates was limited by a lack of detailed information about the absorption cross section. We conclude that our model cross section allows calculations that reproduce atmospheric absorption in this region with a degree of precision that would justify including in the calculation of atmospheric dissociation details such as the Fraunhofer structure and temporal variations in the solar spectrum and seasonal variations in the atmospheric structure.

Acknowledgments. This work was supported by grants from the Australian Research Grants Scheme and the U.S. Air Force Geophysics Laboratory. The authors wish to thank F. A. Smith for valuable assistance in obtaining the experimental data.

The Editor thanks G. Kockarts and R. D. Hudson for their assistance in evaluating this paper.

References

Ackerman, M., F. Biaume, and G. Kockarts, Absorption cross sections of the Schumann-Runge bands of molecular oxygen, Planet. Space Sci., 18, 1639, 1970.

Blake, A. J., An atmospheric absorption model for the Schumann-Runge bands of oxygen, J. Geophys. Res., 84, 3272, 1979.

Fang, T. M., S. C. Wofsy, and A. Dalgarno, Opacity distribution functions and absorption in the Schumann-Runge bands of oxygen, Planet. Space Sci., 22, 413, 1974.

Frederick, J. E., and R. D. Hudson, Dissociation of molecular oxygen in the Schumann-Runge bands, J. Atmos. Sci., 37, 1099, 1980.

Frederick, J. E., R. D. Hudson, and J. E. Mentall, Stratospheric observations of the attenuated solar irradiance in the Schumann-Runge band absorption region of molecular oxygen, J. Geophys. Res., 86, 9885, 1981.

Gies, H. P. F., S. T. Gibson, D. G. McCoy, and A. J. Blake, Experimentally determined oscillator strengths and linewidths for the Schumann-Runge band system of molecular oxygen-III. The (7-0) to (19-0) bands, J. Quant. Radiat. Transfer, 26, 469, 1981.

Gies, H. P. F., S. T. Gibson, A. J. Blake, and D. G. McCoy, The Schumann-Runge continuum of oxygen at wavelengths greater than 175 nm, J. Geophys. Res., 87, 8307, 1982.

Hall, L. A., Solar ultraviolet irradiance at 40 kilometers in the stratosphere, J. Geophys. Res., 86, 555, 1981.

Hudson, R. D., and V. L. Carter, Predissociation in N and O, Can. J. Chem., 47, 1840, 1969.

Kockarts, G., Penetration of solar radiation in the Schumann-Runge bands of molecular oxygen in Mesospheric models and related experiments, edited by G. Fiocco, pp 160-167, D. Reidel, Hingham, Mass., 1971.

Kockarts, G., Absorption and photodissociation in the Schumann-Runge bands of molecular oxygen in the terrestrial atmosphere, Planet. Space Sci., 24, 589, 1976.

Kockarts, G., Effects of solar variations on the upper atmosphere, Solar Phys., 74 295, 1981.

Longmire, M. S., J. D. F. Bartoe, G. M. Brown, G. E. Brueckner, and R. Tousey, Measurements of spectrally integrated atmospheric transmittance in the O Schumann-Runge bands and derived oxygen column densities: 76-102 km, J. Geophys. Res., 84, 1277, 1979.

(Received August 23, 1982;
revised October 4, 1982;
accepted October 15, 1982.)

END

3-87

DTIC